

Convex mixed-integer optimization with Frank-Wolfe methods

Deborah Hendrych

*Freie Universität Berlin, Germany
Zuse Institute Berlin, Germany*

HENDRYCH@ZIB.DE

Hannah Troppens

*Freie Universität Berlin, Germany
Zuse Institute Berlin, Germany*

TROPPENS@ZIB.DE

Mathieu Besançon

Zuse Institute Berlin, Germany

BESANCON@ZIB.DE

Sebastian Pokutta

*Technische Universität Berlin, Germany
Zuse Institute Berlin, Germany*

POKUTTA@ZIB.DE

Abstract

Mixed-integer nonlinear optimization encompasses a broad class of problems that present both theoretical and computational challenges. We propose a new type of method to solve these problems based on a branch-and-bound algorithm with convex node relaxations. These relaxations are solved with a Frank-Wolfe algorithm over the convex hull of mixed-integer feasible points instead of the continuous relaxation via calls to a mixed-integer linear solver as the linear oracle. The proposed method computes feasible solutions while working on a single representation of the polyhedral constraints, leveraging the full extent of mixed-integer linear solvers without an outer approximation scheme and can exploit inexact solutions of node subproblems.

1. Introduction

Mixed-integer nonlinear optimization problems (MINLP) are a challenging class combining both combinatorial structures and nonlinearities which can model a broad range of problems arising in engineering, transportation, and more generally operations and other application contexts. Combinatorial constraints can capture rich properties required for a solution, e.g., solutions that must be a path, cycle, or tour in a graph, or solutions with maximum support or guaranteed sparsity. The dominant algorithmic frameworks for solving such problems are combinations of branch-and-bound (BnB) with spatial and integer branching, and cutting planes added iteratively.

We focus in this paper on mixed-integer convex problems in which the nonlinear constraints and objectives are convex and present a new algorithmic framework for solving these problems that exploit recent advances in so-called Frank-Wolfe (FW) or Conditional Gradient (CG) methods. The problem class we consider is of the type:

$$\min_{\mathbf{x} \in \mathbb{R}^n} f(\mathbf{x}) \text{ s.t. } \mathbf{x} \in \mathcal{X}, \quad (1)$$

where \mathcal{X} is a compact nonconvex set admitting a *boundable linear minimization oracle* (LMO), i.e., a set over which optimizing a linear function can be done efficiently (comparatively to the original problem), even when bounds are added or modified. Formally, we consider we have access to an oracle taking new bounds (\mathbf{l}, \mathbf{u}) and a direction \mathbf{d} :

$$(\mathbf{l}, \mathbf{u}, \mathbf{d}) \in \mathbb{R}^n \times \mathbb{R}^n \times \mathbb{R}^n \rightarrow \operatorname{argmin}_{\mathbf{v} \in \mathbb{R}^n} \langle \mathbf{v}, \mathbf{d} \rangle \text{ s.t. } \mathbf{v} \in \mathcal{X} \cap [\mathbf{l}, \mathbf{u}]. \quad (\text{B-LMO})$$

We assume that one source of nonconvexity of \mathcal{X} stems from integrality constraints and will formalize that requirement in the following section. Given $J \subseteq \{1 \dots n\}$, we will denote:

$$\mathcal{X} = \overline{\mathcal{X}} \cap \mathbb{Z}_J,$$

where $\mathbb{Z}_J = \{\mathbf{x} \in \mathbb{R}^n, \mathbf{x}_j \in \mathbb{Z} \forall j \in J\}$,

with $\overline{\mathcal{X}}$ a continuous relaxation of \mathcal{X} (which is in general not unique). A typical example for \mathcal{X} includes polyhedral and integrality constraints, and combinatorial structures (which we will detail in the following sections). The objective $f : \text{conv}(\mathcal{X}) \rightarrow \mathbb{R}$ is a differentiable Lipschitz-smooth convex function with a gradient accessed as an oracle, i.e., we do not require an expression graph. The proposed framework also extends to nonconvex objectives when the nonconvexity affects only binary variables and exact convexifiers can be built by adding convex terms vanishing on $\{0, 1\}$ (Crama et al., 2022). In the more general case, the framework can be used as a heuristic to compute high-quality solutions.

Several families of MINLP methods have been developed over the last decades, rooted in both nonlinear and discrete optimization approaches; see Kronqvist et al. (2019) for a recent review of methods for convex MINLPs. Some solvers such as Knitro (Byrd et al., 2006) or Couenne (Belotti, 2009) implement a BnB algorithm that solves a nonlinear relaxation at each node of the tree. These subproblems are however expensive: typical algorithms are interior points or sequential quadratic programming, both relying on expensive second-order information and yielding high-accuracy solutions. An alternative family of approaches was introduced in Quesada & Grossmann (1992), solving Linear Programs (LPs) at each node and nonlinear problems only to compute feasible solutions and additional cuts when integer solutions are found. An LP-based method is also at the core of the SCIP (Bestuzheva et al., 2021) MINLP solution process, with additional techniques handling nonconvex nonlinearities. The solvers SHOT (Lundell et al., 2022; Kronqvist et al., 2016) and Pavito.jl (JuMP-dev, 2018) use single-tree polyhedral outer approximation approaches, relying on the Mixed-Integer Programming (MIP) solver to build the main relaxation of the problem, similar to the framework proposed in Bertsimas et al. (2021) for mixed-binary convex problems. Bonmin (Bonami et al., 2008) uses a hybrid approach with both outer polyhedral approximations and BnB. In Chen & Goulart (2022), mixed-integer conic problems are tackled with ADMM using inexact termination and a safe dual bound recovery in a BnB framework. Unlike ADMM, Frank-Wolfe is a primal approach with a lower bound computed at each iteration that can be used to terminate node processing and derive a global tree bound. Furthermore, our LMO-based solver avoids projections onto cones which can be expensive (requiring eigendecompositions) or numerically unstable (for exponential and positive semidefinite cones for instance). It is important to note that in many MINLP solution approaches, nonlinearities are handled through separation (via gradient cuts or supporting hyperplane cuts). Separation is not possible if the nonlinearity is in the objective and most solvers therefore allow for nonlinearities in the constraints only, requiring an epigraph formulation of the objective function losing the initial structure of Problem (1). Some lines of work focused on specialized BnB approaches for some sparse regression or best subset selection problems (Bertsimas et al., 2016; Hazimeh & Mazumder, 2020; Gómez & Prokopyev, 2021; Moreira Costa et al., 2022). These approaches however rely on the properties of the quadratic loss and/or of the constraint set and do not extend to other loss functions (e.g., logistic or Poisson regression), additional constraints (arbitrary linear constraints on the features, grouped subset selection, integer predictor), or other MINLPs of the form (1).

Ideas for warm-starting Frank-Wolfe variants based on the active set representation of the solution (i.e., as a convex combination of vertices) have been explored in the past; in Moondra et al. (2021), an Away-step FW (AFW) variant leveraging active sets from previous iterations in an online optimization setting. In Joulin et al. (2014), FW or variants thereof are called over the integer hull of combinatorial problems, calling a MIP solver as LMO and additional roundings to compute feasible solutions of good quality. The hardness of optimization over the integer hull motivated lazified conditional gradient approaches in Braun et al. (2017). We however generalize lazification techniques to consider the whole tree. BnB with AFW has been explored in Buchheim et al. (2018) for a portfolio problem, each subproblem is solved inexactly to compute lower bounds from the FW gap, each branching performs fixing to all possible values of the integer variable instead of adding bounds. In contrast, we leverage the Blended Pairwise Conditional Gradient (BPCG) algorithm (Tsuji et al.,

2021) which enables us to aggressively reuse information (from computed vertices); its convergence speed is typically higher than AFW while the iterates remain sparser. This sparsity greatly benefits branching as the fractionality of solutions is lower in most cases. We point interested readers to Braun et al. (2022) for a general overview of FW methods.

OUR APPROACH AND CONTRIBUTION

We propose a different solution approach to Problem (1), consisting in a branch-and-bound process over the convex hull of the feasible region with inexact node processing. A key feature is that at each node, FW solves the nonlinear subproblem over the convex hull of integer-feasible solutions or *integer hull* and not over the continuous relaxation. This is allowed by solving a MIP as the LMO within the FW solving process, thus resulting in vertices of the integer hull. No other access to the feasible region (e.g., complete description as linear inequalities) or the objective function (e.g., Hessian information or expression graph) is required. In particular, we do not require epigraph formulations, and we retain the original polyhedral structure; see also Figure 1 for a schematic overview. The central novel elements of our approach are:

1. Instead of solving weaker continuous relaxations at each node of the branch-and-bound tree, we optimize over the convex hull of integer-feasible solutions by solving mixed-integer linear problems in the LMO, obtaining stronger relaxations, several feasible solutions at each node, and reducing the size of the tree;
2. We replace exact convex solvers with a Frank-Wolfe-based error-adaptive solution process, i.e., a solution process for which the amount of computations performed is increasing for higher accuracies;
3. We leverage the active set representation of the solution at each node to warm-start the children iterates and reduce the number of calls to the Mixed-Integer Programming (MIP) solver;
4. We develop new lazification techniques and strong branching strategies for our framework;
5. We exploit the convexity and Frank-Wolfe gap to tighten bounds at each node, further reducing the search space.

One motivation for outer approximation is the ability to leverage a MIP solver through single-tree approaches i.e., the MIP solver is called only once and coordinates the whole solving process with separation callbacks. This approach however carries several issues: only near-feasible and near-optimal solutions are obtained in the limit towards the end of the solution process and rely on MIP heuristics for primal feasible solutions. Furthermore, the separation constraints for the nonlinear feasible set, often linear cutting planes, are in general dense in the variables involved in the nonlinear expressions. These dense cuts slow down the MIP solving process and yield numerically ill-conditioned LP relaxations. We face none of these issues since we do not rely on outer approximations at all but rather on nonlinear relaxations. While this may seem inefficient at first and naive realizations would require a very large number of MIP subproblems to be solved, our framework allows utilizing recent advances in FW and MIP methods to considerably reduce the number of MIP subproblems. Specifically, our method is the first one, to the best of our knowledge, that exploits the flexibility and advances of modern MIP solvers outside polyhedral outer approximation, maintaining feasibility throughout the process.

We complement the above with extensive computational results to demonstrate the effectiveness of our approach. The algorithm is available as a registered Julia package `Boscia.jl`¹ open-sourced under the MIT license.

2. Nonlinear branch-and-bound over integer hulls with linear oracles

In this section, we present the main paradigm for our framework. Our approach is primarily based on branch-and-bound, the feasible region handled at each node is identical except for updated fixings and bounds on the variables that must take integer values. At each node, we solve a convex relaxation with updated local bounds for the integer variables using a FW-based algorithm providing a relaxed primal solution and lower

1. <https://github.com/ZIB-IOL/Boscia.jl>

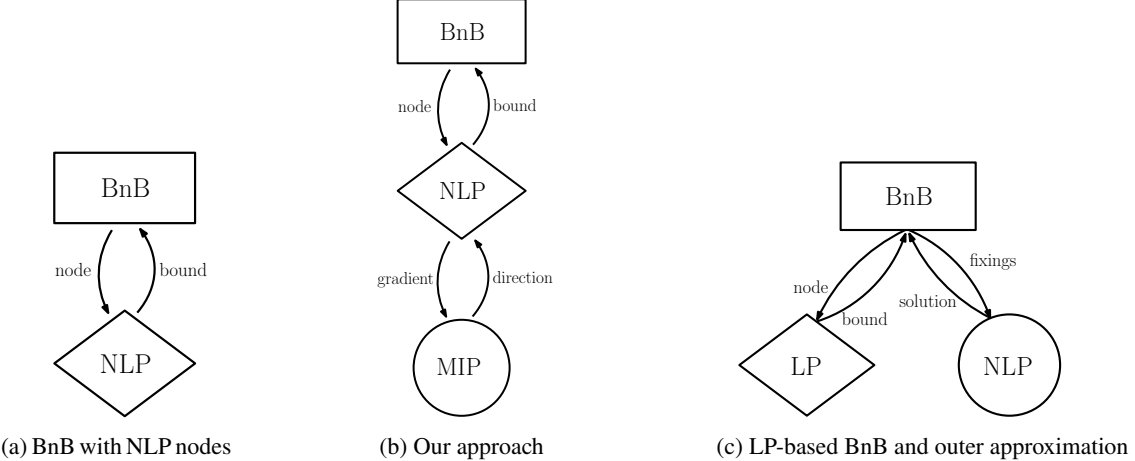


Figure 1: Three main algorithmic frameworks for MINLPs. Diamond blocks represent the nodal relaxations in the given framework. [Figure 1a](#) corresponds to a classic BnB framework on top of NLP relaxations, [Figure 1c](#) represents the mechanism of LP-based MINLP frameworks and outer approximations, [Figure 1b](#) is our proposed approach with the linearized models solved as MIPs within the Frank-Wolfe algorithm on top of which we branch.

bound. This family of algorithms only requires a gradient oracle for the objective function f , and not a full analytical expression nor Hessian information. It accesses the feasible region P through the LMO, which, given a direction \mathbf{d} , solves $\mathbf{v} \leftarrow \operatorname{argmin}_{\mathbf{x} \in P} \langle \mathbf{d}, \mathbf{x} \rangle$, where \mathbf{v} is an extreme point or vertex of the feasible set. This means in particular that the feasible region does not have to be given in closed form, e.g., with constraint matrix and right-hand side, as long as the LMO is well-defined with a suitable algorithm implementing it. Instead of optimizing over the continuous relaxation of Problem (1) with updated bounds at each node, we optimize over the convex hull of feasible solutions at each node. For that purpose, the LMO called within the FW procedure is the MIP solver with bounds updated for the node and objective given by the gradient information at the current solution. This design choice is illustrated in [Figure 2](#).

The main algorithm we propose is presented in [Algorithm 2.1](#), containing at its core a BnB procedure with approximate subproblems. The procedure `near-optimal_relaxation_solve` solves the relaxation to approximate optimality with a specified FW gap and returns a tuple including the relaxation $\hat{\mathbf{x}}$, FW gap g , active and shadow sets \mathcal{A} , \mathcal{S} , and set of primal solutions \mathcal{H} computed through heuristics of our methods or of the MIP solver. More details on the subproblem solution method are provided in Appendix A. `best_bound_node(\mathcal{N})` returns the node with the lowest dual bound.

Constraint representability with integer hulls. Optimizing over the integer hull at each node automatically makes all vertices computed across FW iterations feasible for the original problem. The feasible region itself is tightened, greatly reducing the tree size for problems that have a weak continuous relaxation. This approach also allows us to integrate other nonconvex constraints as long as the integer points of their convex hull respect the combinatorial constraint, an assumption formalized below.

Assumption 1 (non-extreme integer points feasibility). *Let X be the feasible set, \bar{X} its continuous relaxation, $\operatorname{conv}(X)$ the convex hull of X , \mathbb{Z}_J the set of points respecting integrality constraints, and (\mathbf{l}, \mathbf{u}) the local bounds at the node. We assume that:*

$$x \in \operatorname{conv}(X) \cap \mathbb{Z}_J \cap [\mathbf{l}, \mathbf{u}] \Rightarrow x \in X.$$

In other words, there exists no integer point in the convex hull of X which is not feasible.

Algorithm 2.1 Boscia algorithm for Problem (1)

Require: Primal-dual tolerance δ , feasible set \mathcal{X} as a boundable LMO, J the set of integer variables, objective f , initial point \mathbf{v}_0 , FW gap tolerance $\{\varepsilon_t\}_{t \geq 0}$.

- 1: $\mathbf{l}^{(0)}, \mathbf{u}^{(0)} \leftarrow \text{global_bounds}(\mathcal{X})$
- 2: $\hat{\mathbf{x}}^{(0)} \leftarrow \mathbf{v}_0$
- 3: $\text{UB} \leftarrow f(\mathbf{v}_0)$
- 4: $g_0 \leftarrow \max_{\mathbf{v} \in \mathcal{X}} \langle \nabla f(\mathbf{x}_0), \mathbf{v}_0 - \mathbf{v} \rangle$
- 5: $n_0 \leftarrow (\mathbf{l}^{(0)}, \mathbf{u}^{(0)}, \mathcal{A}_0, \mathcal{S}_0, g_0, f(\hat{\mathbf{x}}^{(0)}) - g_0)$
- 6: $\mathcal{N}_0 \leftarrow \{n_0\}$
- 7: $\text{UB} \leftarrow \min\{\text{UB}, \min_{\mathbf{v} \in \mathcal{A}_0 \cup \mathcal{S}_0 \cup \mathcal{H}_0} f(\mathbf{v})\}$
- 8: $\text{LB} \leftarrow f(\hat{\mathbf{x}}^{(0)}) - g_0$
- 9: $t \leftarrow 0$
- 10: **while** $\text{UB} - \text{LB} > \delta$ and $\mathcal{N}_t \neq \emptyset$ **do**
- 11: $n_t \leftarrow \text{best_bound_node}(\mathcal{N}_t)$
- 12: $(\mathbf{l}^{(t)}, \mathbf{u}^{(t)}, \bar{\mathcal{A}}_t, \bar{\mathcal{S}}_t, \bar{g}_t, \bar{b}_t) \leftarrow n_t$
- 13: $\bar{\mathcal{N}}_t \leftarrow \mathcal{N}_t \setminus \{n_t\}$
- 14: $(\hat{\mathbf{x}}^{(t)}, g_t, \mathcal{A}_t, \mathcal{S}_t, \mathcal{H}_t) \leftarrow \text{near-optimal_relaxation_solve}(\mathbf{l}^{(t)}, \mathbf{u}^{(t)}, \bar{\mathcal{A}}_t, \bar{\mathcal{S}}_t, \text{UB}, \varepsilon_t)$
- 15: $\text{UB} \leftarrow \min\{\text{UB}, \min_{\mathbf{v} \in \mathcal{A}_0 \cup \mathcal{S}_0 \cup \mathcal{H}_0} f(\mathbf{v})\}$
- 16: $b_t \leftarrow f(\hat{\mathbf{x}}^{(t)}) - g_t$
- 17: **if** $b_t > \text{UB}$ **then**
- 18: prune suboptimal node
- 19: **else if** $\hat{\mathbf{x}}^{(t)} \in \mathcal{X}$ **then** ▷ integer point, no further branching
- 20: $\text{UB} \leftarrow \min\{\text{UB}, f(\hat{\mathbf{x}}^{(t)})\}$
- 21: close node
- 22: **else** ▷ fractional node to split
- 23: $\hat{\mathbf{l}}^{(t)}, \hat{\mathbf{u}}^{(t)} \leftarrow \text{dual_bound_tightening}(\mathbf{l}^{(t)}, \mathbf{u}^{(t)}, \nabla f(\hat{\mathbf{x}}^{(t)}), \text{UB}, b_t)$
- 24: $j \in \{j \in J \mid \hat{\mathbf{x}}_j^{(t)} \notin \mathbb{Z}\}$ ▷ find variable to branch on
- 25: $\mathbf{l}_r^{(t)} \leftarrow \hat{\mathbf{l}}^{(t)} + \mathbf{e}_j \left(\lceil \hat{\mathbf{x}}_j^{(t)} \rceil - \hat{\mathbf{l}}_j^{(t)} \right)$ ▷ compute bounds for left and right node
- 26: $\mathbf{u}_l^{(t)} \leftarrow \hat{\mathbf{u}}^{(t)} + \mathbf{e}_j \left(\lfloor \hat{\mathbf{x}}_j^{(t)} \rfloor - \hat{\mathbf{u}}_j^{(t)} \right)$
- 27: $\mathcal{A}_l, \mathcal{S}_l, \mathcal{A}_r, \mathcal{S}_r \leftarrow \text{partition_vertices}(\mathcal{A}_t, \mathcal{S}_t, j)$
- 28: $n_l \leftarrow (\mathbf{l}_r^{(t)}, \mathbf{u}_l^{(t)}, \mathcal{A}_l, \mathcal{S}_l, g_t, b_t)$
- 29: $n_r \leftarrow (\mathbf{l}_r^{(t)}, \mathbf{u}_l^{(t)}, \mathcal{A}_r, \mathcal{S}_r, g_t, b_t)$
- 30: $\mathcal{N}_{t+1} \leftarrow \bar{\mathcal{N}}_t \cup \{n_l, n_r\}$
- 31: **end if**
- 32: $t \leftarrow t + 1$
- 33: **end while**

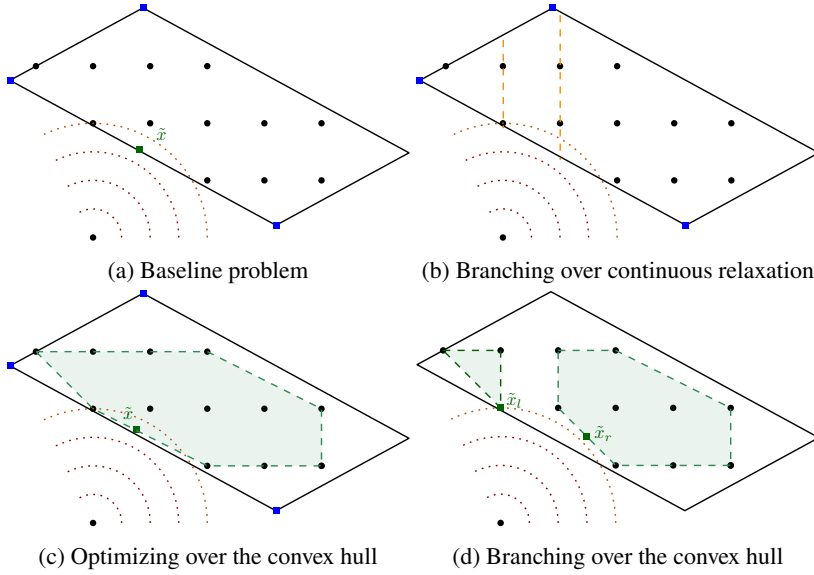


Figure 2: Branching over the convex hull. Figure 2a shows the baseline problem with the level curves of the objective, polyhedron, the optimum over the relaxation \tilde{x} , and examples of potentially active vertices for a near-optimal solution (the top vertex is dropped in an optimal solution). Branching over the continuous relaxation is shown in Figure 2b. Our approach is shown in Figure 2c and Figure 2d, optimizing over the convex hull with the help of the MIP solver. Branching only once results in an optimal solution in the left part in Figure 2d, with the right part being pruned once \tilde{x}_l is found.

Assumption 1 ensures that if the relaxation obtained at a node is integer-feasible, it is feasible for X since it is obtained as a convex combination of extreme points of X intersected with local bounds. On a relaxed solution, the algorithm thus branches if $x \notin X$ or closes the node with an admissible solution, it cannot terminate on an integer point that would not be feasible for X , ensuring its exactness and global convergence.

We illustrate this condition with two families of constraints that respect this condition and one that does not. Indicator constraints are nonconvex constraints of the form $(z, \mathbf{x}) \in \{0, 1\} \times \mathbb{R}^n : z = 1 \Rightarrow \langle \mathbf{a}, \mathbf{x} \rangle \leq b$. They can represent, among others, logical, disjunctive, or SOS1 constraints and are crucial in MIP and MINLP applications (Bertsimas et al., 2021). Vertices of the integer hull respect the binary condition, thus $z \in \{0, 1\}$ on a vertex. If for a given solution, vertices of the active set all have $z = 0$ or all have $z = 1$, the indicator constraint is respected; otherwise, the relaxed solution \hat{z} is fractional and will be branched on. This means that our framework natively handles indicator constraints by branching on the binary variable only. This extends to indicators with convex functions or *convex superindicator* expressed as:

$$(z, \mathbf{x}) \in \{0, 1\} \times \mathbb{R}^n : z = 1 \Rightarrow g(\mathbf{x}) \leq 0$$

with $g(\cdot)$ convex. Indeed, vertices are feasible by definition, so $z = 0$ or $z = 1$, $g(\mathbf{v}) \leq 0$ for any vertex \mathbf{v} in the active set. If $z = 1$ in the solution, convexity implies that $g(\sum_k \lambda_k \mathbf{v}_k) \leq 0$ with λ_k weights of the vertices in the final convex combination.

Other constraints that are directly representable are logical constraints (or, and, and xor constraints) or more broadly arbitrary constraints of pure binary variables. Although these can typically be represented with linear constraints, most MIP solvers include specialized forms for these which helps presolving, propagation, conflict analysis and separation. Examples of constraints that are not supported directly by our framework are SOS1/SOS2 constraints over non-binary variables or piecewise linear functions, since integrality is not sufficient to ensure feasibility in their convex hull, they would therefore require additional branching or

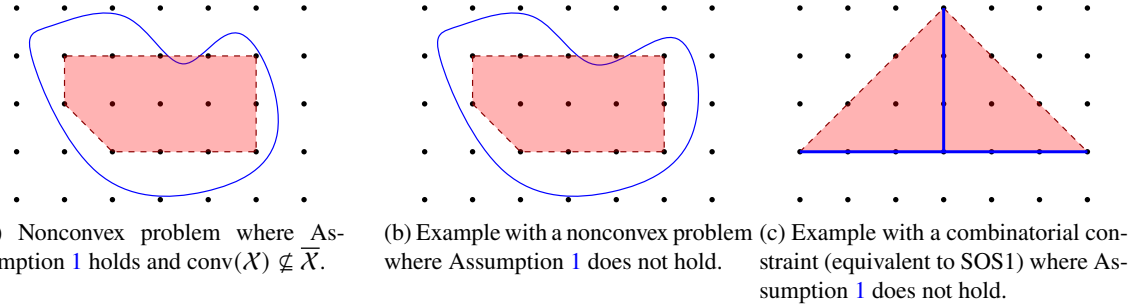


Figure 3: Positive and negative illustrations for Assumption 1. The blue solid curve represents the boundary of \bar{X} , the red dashed shaded area is $\text{conv}(X)$.

reformulations. Our framework can also incorporate nonlinear constraints in the feasible set X , as long as Assumption 1 is respected. From the computational perspective however, we must note that this makes sense only if the LMO subproblems remain inexpensive compared to the original problem. We illustrate examples where Assumption 1 may or may not hold in Figure 3.

Blended Pairwise Conditional Gradient (BPCG). The classic FW algorithm calls an LMO once per iteration. Even though this is acceptable in contexts where the LMO is inexpensive compared to gradient evaluations or in large dimensions in which storage of vertices is an issue, it is not the best suited one when optimizing over polytopes. The first reason is the descent direction which can be significantly misaligned with the negative of the gradient. The second and essential one in our context is that the LMO is particularly expensive (consisting of solving a MIP). Instead, we employ methods that exploit the *active set* decomposition of the iterate \mathbf{x} , i.e., its representation as a convex combination of vertices obtained from the LMO $\mathbf{x}_t := \sum_k \lambda_k \mathbf{v}_k$. Typical algorithms leveraging this representation are the Away Frank-Wolfe, Pairwise Conditional Gradient, and Blended Conditional Gradient algorithms (Guélat & Marcotte, 1986; Lacoste-Julien & Jaggi, 2015; Braun et al., 2019). The variant we focus on is the recently-proposed Blended Pairwise Conditional Gradient (BPCG) algorithm (Tsuji et al., 2021) which blends Frank-Wolfe steps in which a vertex is added to the active set with pairwise steps which do not require any LMO call and only perform inner products between vertices and the gradient. Empirically, BPCG produces iterates with a smaller active set across all iterations compared to other FW algorithms. We use more specifically a modification of the lazified BPCG from (Tsuji et al., 2021) implemented in `FrankWolfe.jl`; the algorithm is presented in detail in the supplement.

Active and shadow set branching. We accelerate the solving process of individual nodes through warm starts. At the end of each BPCG call, the optimal solution is given as a convex combination of vertices in an active set. All these vertices are obtained by calls to the LMO and are thus extreme points of the integer hull. When branching, the vertices can be partitioned to form starting active sets for the left and right children. As the relaxed solution is fractional in the variable branched on, it always contains at least one vertex for each of the children. The weights are also transferred to each child for the corresponding vertex and renormalized. BPCG can also drop vertices from the active set, in a single run of the algorithm, a dropped vertex is not part of the optimal active set and will not be re-added. However, we solve subproblems across different nodes. As such, a dropped vertex can be relevant for another subproblem further down the tree when the bounds have been updated, adding computational burden by redundant calls to the LMO. We therefore maintain a *shadow set*, i.e., a set of discarded vertices collected within each node when they are removed from the active set. The shadow set can be partitioned in a fashion similar to the active set. At all non-root nodes, an extra-lazification layer is added to BPCG: if no suitable pair of vertices can be found in the pairwise step, the algorithm searches the shadow set for a vertex with a suitable inner product with the gradient, using identical criteria as in the lazy BPCG algorithm. Only if this additional step fails does the algorithm perform an LMO call computing

a new vertex. By propagating both the active and shadow set, we significantly reduce the number of calls to the LMO, ensuring we never recompute a given vertex twice within a run for our algorithm.

3. Branch-and-bound techniques for error-adaptive convex relaxations

In this section, we present the techniques derived from branch-and-bound techniques that can be used in our framework. In particular, we highlight the advantages of the error-adaptivity of BPCG, i.e., the property of the computational cost decreasing gradually when the error tolerance increases, and how the various components of modern MIP solvers can be used to enhance the higher-level branch-and-bound process. MIP solvers are implementations of complex algorithms with several key components including presolving, heuristics, bound tightening, and conflict analysis. This is usually also a main motivation for single-tree MINLP solvers handling nonlinearities as a special case of separation within a MIP solving process. We can however also leverage this additional information about the feasible set within our framework by transferring it across nodes.

FW gap-based termination. Frank-Wolfe methods produce at each iteration a primal feasible iterate and a so-called FW gap upper-bounding the optimality gap. They feature many inexpensive iterations (unlike e.g., interior points which require few expensive iterations), with a dual bound gradually increasing with iterations. We leverage this fact to adapt the solving process at each node. Whenever the dual bound reaches the objective value of the best incumbent (or becomes close to the gap tolerance), the node can be terminated early. A significant part of the solving process can be avoided in this manner which is not necessarily the case when nodes are processed with other nonlinear solvers. Pushing this further, the solution process of a node can be stopped at any point to produce a dual bound, even if the solution is not an exact but approximate optimum. The only strict requirement is that the dual bound after solving the current node becomes high enough to yield progress in the overall tree dual bound.

Tree state-dependent termination and evolving error. We implement additional termination criteria for node processing which do not guarantee the node should be pruned but that save on the total number of iterations. One of them is the number of open nodes with a lower bound (obtained from the parent) that is lower than the dual bound of the node being processed during the BPCG run. This set of more promising nodes will be processed before the children of the current node are. If the number of these more promising nodes is high enough, there is a higher probability for the children of the current node not to be processed at all, for instance if an incumbent is found elsewhere that prunes them. We also add an adaptive Frank-Wolfe gap criterion, increasing the precision with the depth in the BnB tree: $\varepsilon_n = \varepsilon_0 \rho^n$, with $\rho \in]0, 1]$ where n is the depth of the current node, starting from the root at depth 0, and clipping when reaching a sufficient depth. With some convex solvers, using a reduced precision could slow down the search, as approximate solutions might exhibit a much higher fractionality when a weaker stopping criterion is used, requiring more branching. In the case of BPCG however, the iterates are a convex combination of few integer extreme points. Furthermore, if the optimal solution at a node is an extreme point itself, the process converges rapidly by dropping the other extreme points from the active set once the optimal one has been added. As such, solutions obtained from low-precision runs do not necessarily exhibit a higher fractionality.

Strong branching. When tackling large discrete problems, the choice of variables to branch on can yield drastic differences in how fast the lower and upper bounds evolve and the overall size of the branch-and-bound tree. A powerful technique to estimate the lower bound increase when branching on a given variable is *strong branching* which solves the children subproblems of a given node for all candidate variables, selecting the variable to branch on that improves the lowest lower bound across children. Other techniques like pseudo-cost branching or recent machine learning approaches try to construct surrogate models to avoid solving the multiple convex subproblems induced by strong branching (Nair et al., 2020).

We propose a new family of branching techniques that leverage the properties of FW algorithms to obtain a partial estimate of the lower bound improvement while greatly reducing the cost. In our context, strong branching with nonlinear subproblems over the integer hull would be too costly to perform variable selection. However, we can (a) relax the strong branching over the integer hull to the continuous relaxation (solving LPs for the LMO instead of MIPs), (b) run few iterations of the subproblem (and/or set a very high FW gap

tolerance). In the limit case, on the one extreme end this corresponds to performing a single FW iteration for the strong branching estimation and the optimal value of a single linear problem is used to select the branching variable. On the other extreme end the complete high-accuracy solve would correspond to using the continuous relaxation of the node. By carefully limiting the precision we can interpolate between these two regimes.

Dual fixing and tightening. In a lot of subproblems, many variables are at their (local) bounds. We can then leverage convexity and primal solutions to deduce safe *dual fixings* or at least *dual tightening* of the bounds, a procedure originally established for MIPs going back to Dantzig (see (Grötschel & Nemhauser, 2008); see also (Achterberg et al., 2020)) and extended to mixed-integer conic problems in Gally et al. (2018) or MINLPs in Mahajan et al. (2021). Dual fixing in these frameworks is a presolving technique, applied in a static manner to a problem to reduce its size before the solving phase. Our approach is slightly different though as we do not explicitly use dual solutions as customary but rather convexity of the objective and availability of the FW gap. These connect to a property of Frank-Wolfe methods developed in Braun & Pokutta (2021), namely that for every Frank-Wolfe vertex \mathbf{v} in a polytope, the dual gap is equal to the inner product of the dual variables with the slack of the polytope, in the case dual solutions exists. Our approach is more general and even works when dual solutions are not readily available e.g., when the LMO is given via a MIP. We confine ourselves here to tightening the upper bound (potentially fixing it to the lower bound); the case for tightening the lower bound is analogous.

Theorem 1. *Let us assume that the bounds are $[\mathbf{l}, \mathbf{u}] \supseteq \mathcal{X}$ and that we have a relaxed solution $\mathbf{x}^{(t)}$ and a variable $j \in J$ such that $\mathbf{x}_j^{(t)} = \mathbf{l}_j$ and $\nabla f(\mathbf{x}^{(t)})_j \geq 0$. Then, if there exists $M \in \{1, \dots, \mathbf{u}_j - \mathbf{l}_j\}$, such that:*

$$M \nabla f(\mathbf{x}^{(t)})_j > \text{UB} - f(\mathbf{x}^{(t)}) + g(\mathbf{x}^{(t)}) \quad (2)$$

with $g(\cdot)$ the Frank-Wolfe gap:

$$g(\mathbf{x}) := \max_{\mathbf{x} \in \mathcal{X}} \left\langle \nabla f(\mathbf{x}^{(t)}), \mathbf{x}^{(t)} - \mathbf{x} \right\rangle,$$

then the upper bound can be tightened to $\mathbf{x}_j^{(t)} \leq \mathbf{l}_j + M - 1$.

Proof. By convexity:

$$\left\langle \nabla f(\mathbf{x}^{(t)}), \mathbf{x} - \mathbf{x}^{(t)} \right\rangle \leq f(\mathbf{x}) - f(\mathbf{x}^{(t)}) \quad \forall \mathbf{x} \in \mathcal{X}.$$

If $\mathbf{x}_j > \mathbf{l}_j$, we can rewrite $\mathbf{x}_j = \mathbf{l}_j + M$, with $M \in \{1, \dots, \mathbf{u}_j - \mathbf{l}_j\}$.

$$\begin{aligned} & (\mathbf{x} - \mathbf{x}^{(t)})_j \nabla f(\mathbf{x}^{(t)})_j + \sum_{k \neq j} \nabla f(\mathbf{x}^{(t)})_k (\mathbf{x} - \mathbf{x}^{(t)})_k \\ &= M \nabla f(\mathbf{x}^{(t)})_j + \sum_{k \neq j} \nabla f(\mathbf{x}^{(t)})_k (\mathbf{x} - \mathbf{x}^{(t)})_k \leq f(\mathbf{x}) - f(\mathbf{x}^{(t)}) \quad \forall \mathbf{x} \in \mathcal{X} \end{aligned}$$

Let us denote $\mathcal{X}_M := \{\mathbf{x} \in \mathcal{X} \mid \mathbf{x}_j \geq \mathbf{l}_j + M\}$ for $M \in \{1, \dots, \mathbf{u}_j - \mathbf{l}_j\}$. Taking the minimum over all solutions $\mathbf{x} \in \mathcal{X}_M$, we obtain:

$$\begin{aligned} \min_{\mathbf{x} \in \mathcal{X}_M} f(\mathbf{x}) - f(\mathbf{x}^{(t)}) &\geq \min_{\mathbf{x} \in \mathcal{X}_M} \mathbf{x}_j \nabla f(\mathbf{x}^{(t)})_j + \min_{\mathbf{x} \in \mathcal{X}_M} \sum_{k \neq j} \nabla f(\mathbf{x}^{(t)})_k (\mathbf{x} - \mathbf{x}^{(t)})_k \\ &= M \nabla f(\mathbf{x}^{(t)})_j - \max_{\mathbf{x} \in \mathcal{X}_M} \sum_{k \neq j} \nabla f(\mathbf{x}^{(t)})_k (\mathbf{x}^{(t)} - \mathbf{x})_k \\ &\geq M \nabla f(\mathbf{x}^{(t)})_j - \max_{\mathbf{x} \in \mathcal{X}} \sum_{k \neq j} \nabla f(\mathbf{x}^{(t)})_k (\mathbf{x}^{(t)} - \mathbf{x})_k. \end{aligned}$$

The last inequality holds since $\mathcal{X}_M \subseteq \mathcal{X}$. Since:

$$\min_{\mathbf{x} \in \mathcal{X}} \nabla f(\mathbf{x}^{(t)})_j (\mathbf{x} - \mathbf{x}^{(t)})_j = 0,$$

we can extend the sum to all variables:

$$\begin{aligned} \min_{\mathbf{x} \in \mathcal{X}_M} f(\mathbf{x}) - f(\mathbf{x}^{(t)}) &\geq M \nabla f(\mathbf{x}^{(t)})_j - \max_{\mathbf{x} \in \mathcal{X}} \langle \nabla f(\mathbf{x}^{(t)}), \mathbf{x}^{(t)} - \mathbf{x} \rangle \\ &= M \nabla f(\mathbf{x}^{(t)})_j - g(\mathbf{x}^{(t)}), \end{aligned}$$

with $g(\cdot)$ is the Frank-Wolfe gap:

$$g(\mathbf{x}) := \max_{\mathbf{x} \in \mathcal{X}} \langle \nabla f(\mathbf{x}^{(t)}), \mathbf{x}^{(t)} - \mathbf{x} \rangle.$$

If the optimal solution is in \mathcal{X}_M , then:

$$\text{UB} - f(\mathbf{x}^{(t)}) \geq \min_{\mathbf{x} \in \mathcal{X}} f(\mathbf{x}) - f(\mathbf{x}^{(t)}) = \min_{\mathbf{x} \in \mathcal{X}_M} f(\mathbf{x}) - f(\mathbf{x}^{(t)}) \geq M \nabla f(\mathbf{x}^{(t)})_j - g(\mathbf{x}^{(t)}), \quad (3)$$

with UB the best primal value. Therefore, if (3) does not hold, i.e.:

$$M \nabla f(\mathbf{x}^{(t)})_j > \text{UB} - f(\mathbf{x}^{(t)}) + g(\mathbf{x}^{(t)}),$$

we can deduce $\mathbf{x}_j \leq \mathbf{l}_j + M - 1$. \square

We exploit [Theorem 1](#) in two ways within our algorithm. First, we strengthen the local bounds at nodes, using the final relaxed solution. Because we incrementally add bounds on integer variables as the algorithm runs further down in the tree, more variables terminate at their bounds, leading to further fixings. We note that tightening reduces the upper bound when a variable is at its lower bound, which implies that all vertices of the active set are at the same bound, and that the active set vertices can be partitioned as described in [Section 2](#), unlike shadow set vertices which may be discarded by the tightening. Tightening not only reduces the number of nodes to solve the problem but may also accelerate LMO calls through the reduction of the integer variable domains. We also provide a stronger version when a strong convexity constant μ is known for the objective in [Theorem 2](#) of [Appendix B](#).

Second, we exploit the root-node relaxation $\bar{\mathbf{x}}$, for which we store the gradient $\nabla f(\bar{\mathbf{x}})$ and the dual bound $f(\bar{\mathbf{x}}) - g(\bar{\mathbf{x}})$. Whenever the upper bound decreases with a new primal solution, we can verify whether the inequality (2) holds and create a set of tighter bounds that are used to preemptively prune out nodes.

Strong convexity bound improvement. For several important classes of problems, a strong convexity parameter μ is known for the objective. In such cases, we can exploit the minimum increase of the objective from a current fractional solution $\hat{\mathbf{x}}$ to preemptively prune nodes or increase their bound. We will illustrate this by branching down on (i.e., flooring) the fractional variable j . The same reasoning applies when branching up (i.e., ceiling). Let us note \mathbf{x}_l^* the optimal solution of the subproblem created after branching on the variable, and $\hat{J} \subseteq J \setminus \{j\}$ the set of other integer variables at fractional values. Our goal is to derive a lower bound for $f(\mathbf{x}_l^*)$ which potentially allows us to prune the node.

$$\begin{aligned} f(\mathbf{x}_l^*) &\geq f(\hat{\mathbf{x}}) + \frac{\mu}{2} \|\mathbf{x}_l^* - \hat{\mathbf{x}}\|_2^2 + \langle \nabla f(\hat{\mathbf{x}}), \mathbf{x}_l^* - \hat{\mathbf{x}} \rangle \\ &\geq f(\hat{\mathbf{x}}) + \frac{\mu}{2} (\hat{\mathbf{x}}_j - \lfloor \hat{\mathbf{x}}_j \rfloor)^2 + \frac{\mu}{2} \sum_{k \in \hat{J}} \min \{(\hat{\mathbf{x}}_k - \lfloor \hat{\mathbf{x}}_k \rfloor)^2, (\lceil \hat{\mathbf{x}}_k \rceil - \hat{\mathbf{x}}_k)^2\} - \langle \nabla f(\hat{\mathbf{x}}), \hat{\mathbf{x}} - \mathbf{x}_l^* \rangle \\ &\geq f(\hat{\mathbf{x}}) + \frac{\mu}{2} (\hat{\mathbf{x}}_j - \lfloor \hat{\mathbf{x}}_j \rfloor)^2 + \frac{\mu}{2} \sum_{k \in \hat{J}} \min \{(\hat{\mathbf{x}}_k - \lfloor \hat{\mathbf{x}}_k \rfloor)^2, (\lceil \hat{\mathbf{x}}_k \rceil - \hat{\mathbf{x}}_k)^2\} - \max_{\mathbf{v} \in \mathcal{X}} \langle \nabla f(\hat{\mathbf{x}}), \hat{\mathbf{x}} - \mathbf{v} \rangle \\ &= f(\hat{\mathbf{x}}) + \frac{\mu}{2} (\hat{\mathbf{x}}_j - \lfloor \hat{\mathbf{x}}_j \rfloor)^2 + \frac{\mu}{2} \sum_{k \in \hat{J}} \min \{(\hat{\mathbf{x}}_k - \lfloor \hat{\mathbf{x}}_k \rfloor)^2, (\lceil \hat{\mathbf{x}}_k \rceil - \hat{\mathbf{x}}_k)^2\} - g(\hat{\mathbf{x}}). \end{aligned}$$

We also note that the strong convexity parameter can be computed only on the integer variables, which can result in a stronger value of μ than on the whole function. Furthermore, strongly convex terms can be added to binary variables when they do not change the value of f on $\{0, 1\}$, for instance by replacing a linear expression $\sum_i \mathbf{c}_i \mathbf{x}_i$ with $\mathbf{c} \geq 0$ by a quadratic one $\sum_i \mathbf{c}_i \mathbf{x}_i^2$.

The obtained improved bounds have several use cases; they can be used directly to find a branching decision removing one of the two branches or maximizing a lower bound on the improvement. Given the form of the inequality, the branching decision maximizing the lower bound improvement is equivalent to most fractional branching. We can also increase the lower bound of the node as the maximum of the bound improvement over all variables (i.e., the bound obtained from the most fractional branching).

The technique is complementary to dual bound tightening: dual bound tightening can be leveraged when a variable is at one of its bounds, tightening the variable domain, while strong convexity improves the dual bound based on fractional variables. A more generic version of the technique only assuming *sharpness* (Hölderian error bound) of the function is developed in Appendix B.

4. Computational experiments

We use the `FrankWolfe.jl` framework (Besançon et al., 2022) to solve the node subproblems. All features specific to our BnB framework are implemented in the open-source Julia package `Boscia.jl`. The BnB core structures are implemented in `Bonobo.jl` and `Boscia.jl` supports all MIP solvers through `MathOptInterface` (Legat et al., 2022). The underlying MIP solver used in the experiments is `SCIP v8.0.2` (Bestuzheva et al., 2021) run single-threaded, strong branching uses `HiGHS v1.2.2` (Huangfu & Hall, 2018) as the LP solver. All experiments were carried out on an 8-core compute node equipped with an Intel Xeon E3-1245v5 3.50GHz CPU and 32GB RAM. We use Julia 1.7.0. The package versions used are `FrankWolfe.jl` v.0.2.15, `Bonobo.jl` v0.1.2, `SCIP.jl` v0.11.8.

Problem classes These problems and additional examples are available in the package repository.

Sparse regression problems. Sparsity is a desirable property for prediction models for reasons of robustness, explainability, computational efficiency or other underlying motivation. Our framework allows for solving all cardinality-constrained regression models including linear regression, sparse Poisson regression, and logistic regression, as long as the loss function is convex and its gradient available. We also experiment with regression models where the predictor coefficients themselves are constrained to take integer values.

The flexible computational model further allows for richer constraint structures encoding more domain knowledge than sparsity alone. In particular, we can encode group sparsity and constraints similar to group lasso (Friedman et al., 2010). Another example of constraint structure we can directly encode is thresholded or two-tailed cardinality-constrained optimization as considered in Ahn et al. (2022): given a compact convex set \mathcal{X} , a convex loss f and a cardinality penalty λ , the tailed cardinality-penalized model they propose is:

$$\min_{\mathbf{x} \in \mathcal{X}} f(\mathbf{x}) + \lambda \|\max\{|\mathbf{x}_i| - \tau_i, 0\}_{i \in [n]}\|_0 + \mu \|\mathbf{x}\|_2^2$$

which can be reformulated using indicator constraints as:

$$\begin{aligned} \min_{\mathbf{x}, \mathbf{z}, \mathbf{s}} \quad & f(\mathbf{x}) - \lambda \sum_i \mathbf{z}_i + \mu \|\mathbf{x}\|_2^2 \\ \text{s.t. } & \mathbf{z}_i = 1 \Rightarrow \mathbf{s}_i \leq 0 \\ & \mathbf{s}_i \geq \mathbf{x}_i - \tau_i \\ & \mathbf{s}_i \geq -\mathbf{x}_i - \tau_i \\ & \mathbf{x} \in \mathcal{X}, \mathbf{z} \in \{0, 1\}^n, \mathbf{s} \in \mathcal{X} \cap \mathbb{R}_+^n. \end{aligned} \tag{TCMP}$$

When the indicator variable \mathbf{z}_i equals one and the slack \mathbf{s}_i are zero, \mathbf{x}_i is constrained in the interval $[-\tau_i, \tau_i]$, the model hence penalizes the number of predictor values above a threshold in absolute value, while ignoring all smaller values. We can provide guaranteed optimal, near-optimal solutions, relaxations and

bounds for Problem (TCMP) or a cardinality-constrained version without additional assumptions, replacing the complementarity constraints of Ahn et al. (2022) with polyhedral and combinatorial constraints.

Sparse coding with permutation matrices. We consider the problem of finding a convex combination of K permutation matrices that approximate an $n \times n$ doubly-stochastic matrix \hat{X} :

$$\min_{X_i \in P_n, \theta \in \Delta_k} \left\| \sum_{i \in [k]} \theta_i X_i - \hat{X} \right\|^2,$$

where Δ_k is the k -dimensional probability simplex, $[k]$ represents the set of integers from 1 to k , and P_n is the set of $n \times n$ permutation matrices. We can convexify the objective with auxiliary variables using bounds on θ and X , and the fact that one of the variables of the bilinear terms is always binary:

$$\min_{X_i \in P_n, \theta \in \Delta_k, Y_i \in \mathbb{R}^{n \times n}} \left\| \sum_{i \in [k]} Y_i - \hat{X} \right\|^2 \text{ s.t. } 0 \leq Y_i \leq X_i, 0 \leq \theta_i - Y_i \leq 1 - X_i.$$

This problem or variants have been considered in Valls et al. (2021); Dufossé & Uçar (2016). It can be viewed as a cardinality-constrained version of sparse coding over the Birkhoff polytope.

Portfolio optimization. We revisit the example of Buchheim et al. (2018), selecting a portfolio with budget b , integrality requirements on shares for some assets, and with a generic convex differentiable risk penalty term $h(\cdot)$:

$$\min_{\mathbf{x}} h(\mathbf{x}) \mathbf{x}^T M \mathbf{x} - \langle r, \mathbf{x} \rangle \text{ s.t. } \langle c, \mathbf{x} \rangle \leq b, \mathbf{x}_j \in \mathbb{Z} \forall j \in J.$$

MIPLIB instances. We take instances from the MIPLIB (Gleixner et al., 2021) with a bounded feasible region and set a convex quadratic objective that minimizes the sum of distances to several vertices. This ensures a sufficient curvature and a continuous optimum in the interior, avoiding a single MIP call to be optimal.

Results

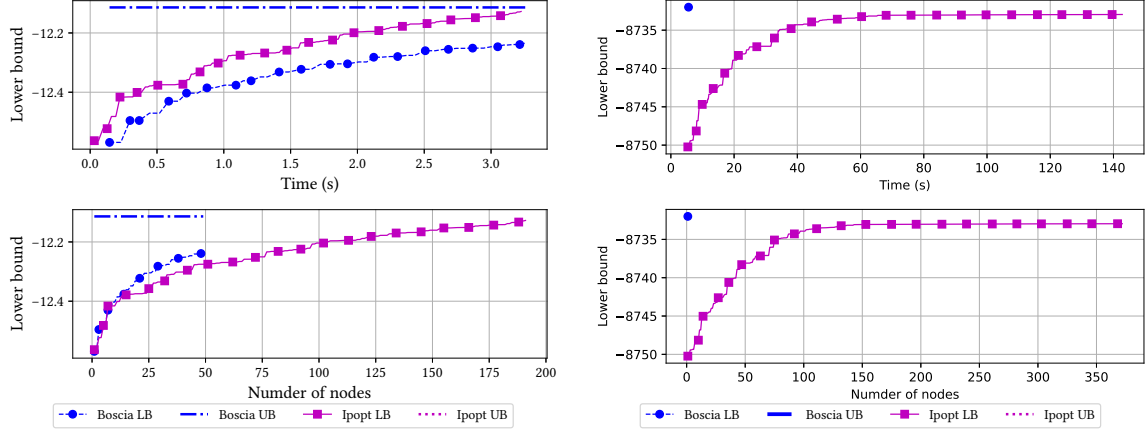
We first present a comparison of our approach with a nonlinear BnB implementation using the Ipopt interior point solver on some MIPLIB instances and set a time limit of 1800 seconds in Figure 4.

Two representative examples of primal-dual convergence on the BnB tree are shown in Figure 5 with, in Figure 5a, a cardinality-constrained linear regression, and in Figure 5b, the permutation matrix coding, exhibiting two different profiles. On the sparse regression, the optimal primal is found early in the search process thanks to the MIP heuristics and vertices, the process could be stopped much earlier with a non-zero dual gap but a high-quality (most of the time optimal) primal solution. On the contrary in Figure 5b, the primal bound continuously improves throughout the run, hinting that better problem-specific heuristics could be applied.

A comparison of branching strategies on a sparse regression problem is presented in Figure 6. On some problems, strong and hybrid strong branching provide a significant speed-up, especially early in the branching process. We also observe that the FW gap tolerance used for strong branching does not influence the progress per node or time significantly. This is likely due to the highly lazified nature of BPCG which performs few LMO calls mostly at the beginning of the strong branching subproblem. A lower gap tolerance would therefore not require more LMO calls but also provide little changes in prediction on the variable to branch on. This limited effect can be explained by the fact that strong branching only provides rankings of the variables based on the obtained bound, high precision is therefore useless as long as the ranking is stabilized.

We assess the advantage provided by using warm starts on the active set and shadow set compared to no warm start on the two-tailed sparse logistic regression problem and the mixed-integer portfolio problem in Figure 7. By using warm starts, Boscia solves more instances and requires less time. We also compare Boscia using BPCG and AFW as the underlying convex solver. More details can be found in Table 1 and Table 13 in the appendix.

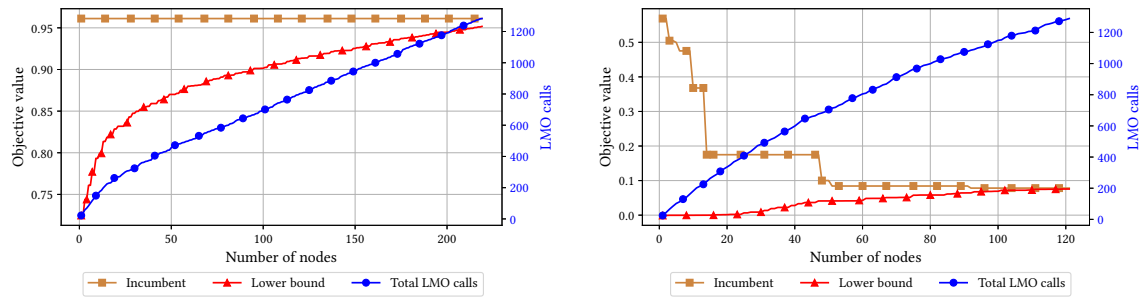
We compare the effect of tightening on the number of LMO calls in Figure 8. On some problems, local and global tightening reduce the number of LMO calls, require fewer nodes and less time, e.g., Figure 36 in



(a) Primal-dual convergence comparison between Boscia and Ipopt for the MIP neos5 example.

(b) Primal-dual convergence comparison between Boscia and Ipopt for the MIP 22433 example. Ipopt has not found an integral leaf hence its upper bound is infinity for the entire run.

Figure 4: Primal-dual convergence comparison between Boscia and Ipopt on MIPLIB instances.



(a) Convergence plot for a linear sparse regression example with a starting root node FW tolerance of 10^{-3} .

(b) Primal-dual progress on the permutation matrices example with $n = 3, k = 2$. The cumulative number of LMO calls per node is displayed to highlight the decrease throughout the tree.

Figure 5: Example of primal-dual convergence runs on sparse linear regression and permutation matrix coding instances.

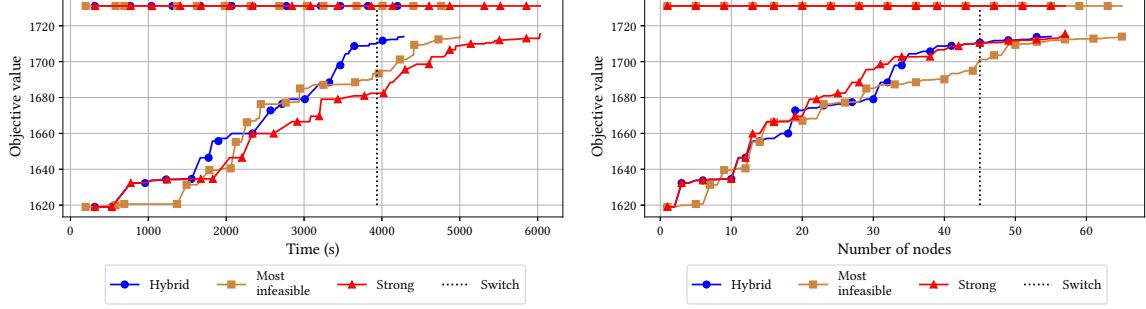
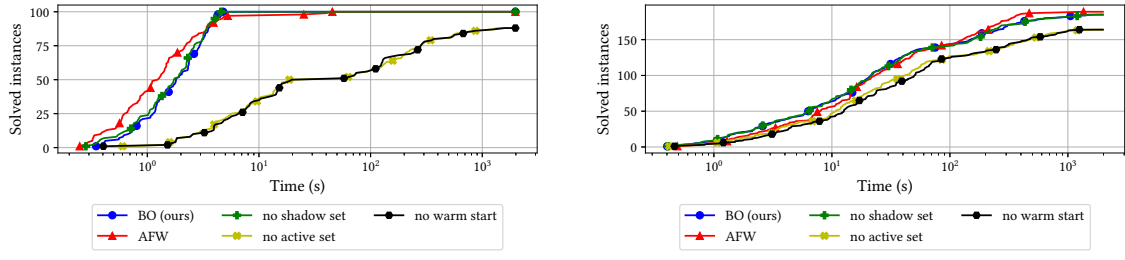


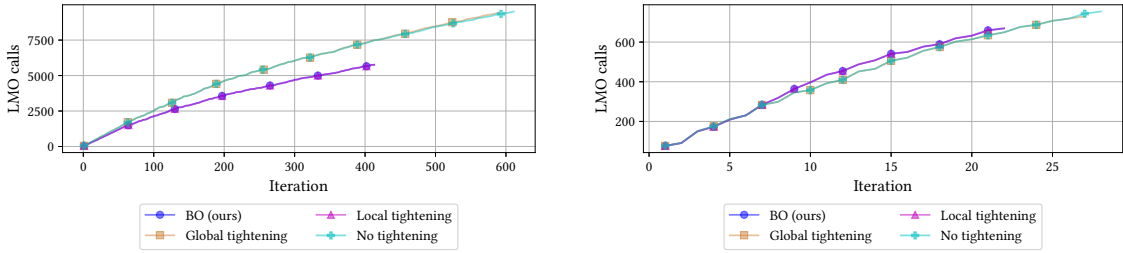
Figure 6: Comparison of branching strategies on an integer sparse regression example with dimension 40. Hybrid branching performs partial strong branching up to depth 5 in the tree, the “switch” limit corresponds to the last call to strong branching by the hybrid strategy. Partial strong branching uses a FW gap of 10^{-3} and at most 10 FW iterations.



(a) Optimally solved two-tailed sparse logistic regression instances

(b) Optimally solved mixed-integer portfolio instances

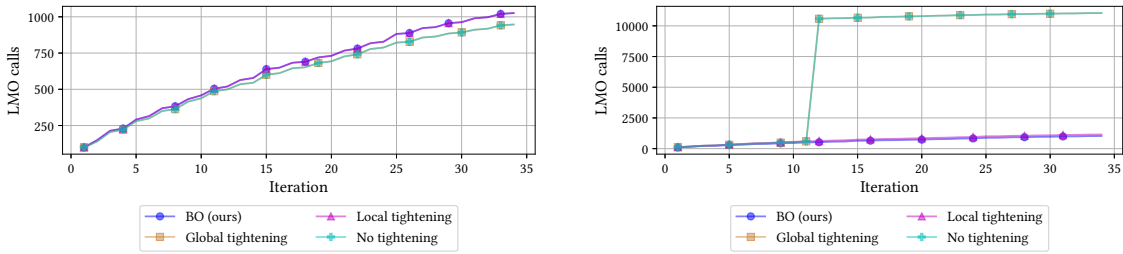
Figure 7: Comparing the number of optimally solved instances of the baseline method (BO) to different warm-start and FW methods of AFW within the time limit of 1800 seconds. Boscia uses the blended pairwise conditional gradient and warm start of the active and shadow sets. AFW uses the Away-step FW and warm start.



(a) Accumulated LMO calls per iteration of different tightening strategies on the sparse regression problem.

(b) Accumulated LMO calls per iteration of different tightening strategies on the mixed portfolio problem.

Figure 8: Comparing the accumulated LMO calls per iteration of different tightening strategies. Boscia applies local and global tightening.



(a) Accumulated LMO calls per iteration with warm start of the shadow set.

(b) Accumulated LMO calls per iteration without warm start of the shadow set.

Figure 9: Comparison of the effect of tightening with and without warm start of the shadow set on the mixed integer portfolio problem. Boscia applies local and global tightening.

the appendix. On other problems as displayed in Figure 9a, tightening can lead to more LMO calls. This is explained by the fact that tightening can render vertices of the shadow set infeasible and discard them, these vertices cannot be used anymore and have to be replaced by new LMO calls on the updated feasible region. If no warm start of the shadow set is used, no tightening requires at least as many LMO calls as Boscia with global and local tightening.

Finally, we compare our framework to an outer approximation method using SCIP with gradient cuts added through a *constraint handler* and the interior-point solver Ipopt. The results for the Poisson regression and the mixed-intger portfolio optimization problems are presented in Figure 10. In the Poisson regression problem, the outer approximation outperforms FW methods for small instances when they can be solved easily, which corresponds to few gradient cuts. Any cut indeed ensures progress bounded away from zero since it removes an integer point, the constraint handler is only called when a new integer candidate is found. In both settings, harder instances make the OA run out of time, our framework solves more instances in the time limit. In addition, our approach solves more instances in the time limit than Ipopt. However, on the mixed-integer portfolio problem, Ipopt outperforms our approach. More details can be found in Table 6 and Table 2 in the appendix.

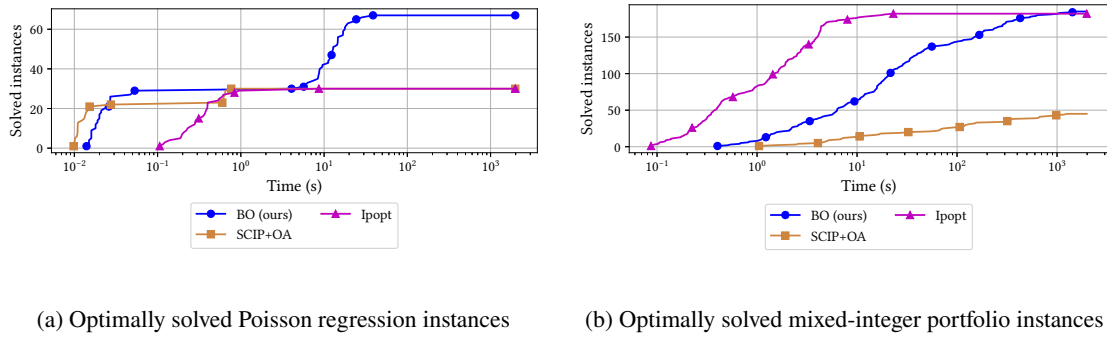


Figure 10: The number of optimally solved instances within the time limit of 1800 seconds and the required time by our solver Boscia, outer approximation with SCIP and the interior point solver Ipopt. An instance is considered optimal if the objective value of the solution is close to the minimal value found by any of the three solvers with an absolute tolerance of $1e-4$ and a relative tolerance of $1e-2$.

5. Conclusion

In this paper, we proposed a novel algorithm for mixed-integer convex optimization relying only on gradient and function evaluations of the objective, and linear optimization over the feasible set. By embedding a FW-based subsolver within a branch-and-bound framework, our method does not rely on separation or projection subproblems. Since FW algorithms rely on LMO calls to handle the constraint set, we significantly strengthen convex relaxations by optimizing over the local integer hull, leveraging the capabilities of modern MIP solvers. Lazification techniques within and across nodes avoid expensive MIP solves by exploiting all vertices that have been discovered and further MIP information, while tightening and stronger dual bounds reduce the size of the branch-and-bound tree and tighten the feasible region.

Acknowledgments

Research reported in this paper was partially supported through the Research Campus Modal funded by the German Federal Ministry of Education and Research (fund numbers 05M14ZAM,05M20ZBM) and the Deutsche Forschungsgemeinschaft (DFG) through the DFG Cluster of Excellence MATH+.

References

- Achterberg, T., Bixby, R. E., Gu, Z., Rothberg, E., and Weninger, D. Presolve reductions in mixed integer programming. *INFORMS Journal on Computing*, 32(2):473–506, 2020.
- Ahn, M., Gangammanavar, H., and Troxell, D. Tractable continuous approximations for constraint selection via cardinality minimization. 2022.
- Belotti, P. CoUEnnE: a user’s manual. 2009.
- Bertsimas, D., King, A., and Mazumder, R. Best subset selection via a modern optimization lens. *The annals of statistics*, 44(2):813–852, 2016.
- Bertsimas, D., Cory-Wright, R., and Pauphilet, J. A unified approach to mixed-integer optimization problems with logical constraints. *SIAM Journal on Optimization*, 31(3):2340–2367, 2021.
- Besançon, M., Carderera, A., and Pokutta, S. FrankWolfe.jl: A High-Performance and Flexible Toolbox for Frank–Wolfe Algorithms and Conditional Gradients. *INFORMS Journal on Computing*, 2022.

- Bestuzheva, K., Besançon, M., Chen, W.-K., Chmiela, A., Donkiewicz, T., van Doornmalen, J., Eifler, L., Gaul, O., Gamrath, G., Gleixner, A., et al. The SCIP Optimization Suite 8.0. *arXiv preprint arXiv:2112.08872*, 2021.
- Bonami, P., Biegler, L. T., Conn, A. R., Cornuéjols, G., Grossmann, I. E., Laird, C. D., Lee, J., Lodi, A., Margot, F., Sawaya, N., and Wächter, A. An algorithmic framework for convex mixed integer nonlinear programs. *Discrete Optimization*, 5(2):186–204, 2008. ISSN 1572-5286. doi: <https://doi.org/10.1016/j.disopt.2006.10.011>. URL <https://www.sciencedirect.com/science/article/pii/S1572528607000448>. In Memory of George B. Dantzig.
- Braun, G. and Pokutta, S. Dual prices for frank–wolfe algorithms. *arXiv preprint arXiv:2101.02087*, 2021.
- Braun, G., Pokutta, S., and Zink, D. Lazifying conditional gradient algorithms. In *International conference on machine learning*, pp. 566–575. PMLR, 2017.
- Braun, G., Pokutta, S., Tu, D., and Wright, S. Blended conditonal gradients. In *International Conference on Machine Learning*, pp. 735–743. PMLR, 2019.
- Braun, G., Carderera, A., Combettes, C. W., Hassani, H., Karbasi, A., Mokthari, A., and Pokutta, S. Conditional gradient methods. *preprint*, 8 2022.
- Buchheim, C., De Santis, M., Rinaldi, F., and Trieu, L. A Frank–Wolfe based branch-and-bound algorithm for mean-risk optimization. *Journal of Global Optimization*, 70(3):625–644, 2018.
- Byrd, R. H., Nocedal, J., and Waltz, R. A. Knitro: An integrated package for nonlinear optimization. In *Large-scale nonlinear optimization*, pp. 35–59. Springer, 2006.
- Chen, Y. and Goulart, P. An early termination technique for ADMM in mixed integer conic programming. In *2022 European Control Conference (ECC)*, pp. 60–65. IEEE, 2022.
- Crama, Y., Elloumi, S., Lambert, A., and Rodriguez-Heck, E. Quadratization and convexification in polynomial binary optimization. 2022.
- Dufossé, F. and Uçar, B. Notes on Birkhoff–von Neumann decomposition of doubly stochastic matrices. *Linear Algebra and its Applications*, 497:108–115, 2016.
- Friedman, J., Hastie, T., and Tibshirani, R. A note on the group lasso and a sparse group lasso. *arXiv preprint arXiv:1001.0736*, 2010.
- Gally, T., Pfetsch, M. E., and Ulbrich, S. A framework for solving mixed-integer semidefinite programs. *Optimization Methods and Software*, 33(3):594–632, 2018.
- Gleixner, A., Hendel, G., Gamrath, G., Achterberg, T., Bastubbe, M., Berthold, T., Christophel, P., Jarck, K., Koch, T., Linderoth, J., et al. MIPLIB 2017: data-driven compilation of the 6th mixed-integer programming library. *Mathematical Programming Computation*, pp. 1–48, 2021.
- Gómez, A. and Prokopyev, O. A. A mixed-integer fractional optimization approach to best subset selection. *INFORMS Journal on Computing*, 33(2):551–565, 2021.
- Grötschel, M. and Nemhauser, G. L. George dantzig’s contributions to integer programming. *Discrete Optimization*, 5(2):168–173, 2008.
- Guélat, J. and Marcotte, P. Some comments on Wolfe’s ‘away step’. *Mathematical Programming*, 35(1):110–119, 1986.
- Hazimeh, H. and Mazumder, R. Fast best subset selection: Coordinate descent and local combinatorial optimization algorithms. *Operations Research*, 68(5):1517–1537, 2020.

- Hoffman, A. J. On approximate solutions of systems of linear inequalities. In *Selected Papers Of Alan J Hoffman: With Commentary*, pp. 174–176. World Scientific, 2003.
- Huangfu, Q. and Hall, J. A. J. Parallelizing the dual revised simplex method. *Mathematical Programming Computation*, 10(1):119–142, 2018. doi: 10.1007/s12532-017-0130-5.
- Hunkenschröder, C., Pokutta, S., and Weismantel, R. Optimizing a low-dimensional convex function over a high-dimensional cube. *arXiv preprint arXiv:2204.05266*, 2022.
- Joulin, A., Tang, K., and Fei-Fei, L. Efficient image and video co-localization with Frank-Wolfe algorithm. In *European Conference on Computer Vision*, pp. 253–268. Springer, 2014.
- JuMP-dev. Pavito, a gradient-based outer approximation solver for convex mixed-integer nonlinear programming, 2018. <https://github.com/jump-dev/Pavito.jl>.
- Kronqvist, J., Lundell, A., and Westerlund, T. The extended supporting hyperplane algorithm for convex mixed-integer nonlinear programming. *Journal of Global Optimization*, 64(2):249–272, 2016.
- Kronqvist, J., Bernal, D. E., Lundell, A., and Grossmann, I. E. A review and comparison of solvers for convex MINLP. *Optimization and Engineering*, 20(2):397–455, 2019.
- Lacoste-Julien, S. and Jaggi, M. On the global linear convergence of Frank-Wolfe optimization variants. *Advances in neural information processing systems*, 28, 2015.
- Legat, B., Dowson, O., Garcia, J., and Lubin, M. MathOptInterface: a data structure for mathematical optimization problems. *INFORMS Journal on Computing*, 2022.
- Lounici, K., Pontil, M., Van De Geer, S., and Tsybakov, A. B. Oracle inequalities and optimal inference under group sparsity. *The annals of statistics*, 39(4):2164–2204, 2011.
- Lundell, A., Kronqvist, J., and Westerlund, T. The supporting hyperplane optimization toolkit for convex MINLP. *Journal of Global Optimization*, pp. 1–41, 2022.
- Mahajan, A., Leyffer, S., Linderoth, J., Luedtke, J., and Munson, T. Minotaur: A mixed-integer nonlinear optimization toolkit. *Mathematical Programming Computation*, 13:301–338, 2021.
- Moondra, J., Mortagy, H., and Gupta, S. Reusing combinatorial structure: Faster iterative projections over submodular base polytopes. *Advances in Neural Information Processing Systems*, 34:25386–25399, 2021.
- Moreira Costa, C., Kreber, D., and Schmidt, M. An alternating method for cardinality-constrained optimization: A computational study for the best subset selection and sparse portfolio problems. *INFORMS Journal on Computing*, 2022.
- Nair, V., Bartunov, S., Gimeno, F., von Glehn, I., Lichocki, P., Lobov, I., O’Donoghue, B., Sonnerat, N., Tjandraatmadja, C., Wang, P., et al. Solving mixed integer programs using neural networks. *arXiv preprint arXiv:2012.13349*, 2020.
- Nemirovskii, A. S. and Nesterov, Y. E. Optimal methods of smooth convex minimization. *USSR Computational Mathematics and Mathematical Physics*, 25(2):21–30, 1985.
- Polyak, B. T. Sharp minima. institute of control sciences lecture notes, moscow, ussr, 1979. In *IIASA workshop on generalized Lagrangians and their applications, IIASA, Laxenburg, Austria*, 1979.
- Quesada, I. and Grossmann, I. E. An LP/NLP based branch and bound algorithm for convex MINLP optimization problems. *Computers & chemical engineering*, 16(10-11):937–947, 1992.
- Tsuji, K., Tanaka, K., and Pokutta, S. Sparser kernel herding with pairwise conditional gradients without swap steps. *arXiv preprint arXiv:2110.12650*, 2021.

Valls, V., Iosifidis, G., and Tassiulas, L. Birkhoff's Decomposition Revisited: Sparse Scheduling for High-Speed Circuit Switches. *IEEE/ACM Transactions on Networking*, 29(6):2399–2412, 2021.

Appendix A. Blended Pairwise Conditional Gradient

We present below the modified Lazy Blended Pairwise Conditional Gradient (L-BPCG) from [Tsuji et al. \(2021\)](#) to solve relaxations at each node. The procedure populates the shadow set with dropped vertices and starts from the warm-started active set. The convergence follows from that of BPCG, we use the same progress measure on whether a shadow vertex offers sufficient decrease as FW direction (vertex the iterates moves towards) as we do for a classic pairwise step. The additional shadow vertex selection can be viewed as a special case of a pairwise step where the initial weight in the active set is zero.

Appendix B. Tighter lower bound and dual tightening inequalities

In this appendix, we provide a modified lower-bound inequality when the function is sharp, and strengthen the dual tightening condition when it is strongly convex.

For many objective functions of interest, strong convexity is too strong of a requirement, if they are not strongly convex or if it offers a loose inequality. We derive an equivalent improved dual bound for functions presenting a *Hölder error bound* or *sharpness* property ([Hoffman, 2003](#); [Nemirovskii & Nesterov, 1985](#); [Polyak, 1979](#)):

Definition 1 (Hölder Error Bound). *Let f be a function $f : X \rightarrow \mathbb{R}$ and C a compact neighborhood around the minimizer set $X^* := \operatorname{argmin}_{\mathbf{x} \in X} f(\mathbf{x})$. The function f satisfies a (θ, M) Hölder Error Bound on C if $\exists \theta \in [0, 1/2]$ and $M > 0$, such that:*

$$\min_{\mathbf{x}^* \in X^*} \|\mathbf{x} - \mathbf{x}^*\| \leq M(f(\mathbf{x}) - f^*)^\theta. \quad (4)$$

We will further assume that the optimum is unique $X^* := \{\mathbf{x}^*\}$. Denoting by \mathbf{x}_l^* the optimal value of the solution after branching, we have:

$$\begin{aligned} \|\mathbf{x}_l^* - \mathbf{x}^*\| &\leq M(f(\mathbf{x}_l^*) - f^*)^\theta \\ f(\mathbf{x}_l^*) &\geq M^{-1/\theta} \|\mathbf{x}_l^* - \mathbf{x}^*\|^{1/\theta} + f(\hat{\mathbf{x}}) - g(\hat{\mathbf{x}}). \end{aligned}$$

Furthermore:

$$\begin{aligned} \|\mathbf{x}_l^* - \mathbf{x}^*\| &\geq \|\mathbf{x}_l^* - \hat{\mathbf{x}}\| - \|\hat{\mathbf{x}} - \mathbf{x}^*\| \\ &\geq \|\mathbf{x}_l^* - \hat{\mathbf{x}}\| - M(f(\hat{\mathbf{x}}) - f^*)^\theta \\ &\geq \|\mathbf{x}_l^* - \hat{\mathbf{x}}\| - M(g(\hat{\mathbf{x}}))^\theta, \end{aligned}$$

resulting in the following bound:

$$f(\mathbf{x}_l^*) \geq M^{-1/\theta} (\|\hat{\mathbf{x}} - \mathbf{x}^*\| - M(g(\hat{\mathbf{x}}))^\theta)^{1/\theta} + f(\hat{\mathbf{x}}) - g(\hat{\mathbf{x}}), \quad (5)$$

where a lower bound on $\|\hat{\mathbf{x}} - \mathbf{x}^*\|$ can be obtained similarly to the strong convexity result. We can also improve the dual bound tightening in case the function is μ -strongly convex.

Theorem 2. *Let us assume that the bounds are $[\mathbf{l}, \mathbf{u}] \supseteq X$ and that we have a relaxed solution $\mathbf{x}^{(t)}$ and a variable $j \in J$ such that $\mathbf{x}_j^{(t)} = \mathbf{l}_j$ and $\nabla f(\mathbf{x}^{(t)})_j \geq 0$. Furthermore, if f is μ -strongly convex, then, if there exists $M \in \{1, \dots, \mathbf{u}_j - \mathbf{l}_j\}$, such that:*

$$M \nabla f(\mathbf{x}^{(t)})_j > \text{UB} - f(\mathbf{x}^{(t)}) + g(\mathbf{x}^{(t)}) - \frac{\mu}{2} M^2, \quad (6)$$

with $g(\cdot)$ the Frank-Wolfe gap:

$$g(\mathbf{x}) := \max_{\mathbf{x} \in X} \langle \nabla f(\mathbf{x}^{(t)}), \mathbf{x}^{(t)} - \mathbf{x} \rangle,$$

then the upper bound can be tightened to $\mathbf{x}_j^{(t)} \leq \mathbf{l}_j + M - 1$.

Algorithm A.1 Lazy Blended Pairwise Conditional Gradient with Shadow Set and Cutoff

Require: Starting active set \mathcal{A}_0 and weights λ , shadow set S_0 , function f , feasible set of current node P , ε_{tol} , accuracy $K \geq 1$, primal bound \hat{f} .

Ensure: Final iterate \mathbf{x} such that $f(\mathbf{x}) \leq f^* + \varepsilon_{\text{tol}}$ or a dual bound greater than \hat{f}

```

1:  $\mathbf{x}_0 \leftarrow \sum_{k=1}^{|\mathcal{A}_0|} \lambda_k \mathbf{v}_k$ 
2:  $\Phi_0 \leftarrow \max_{\mathbf{v} \in P} \langle \nabla f(\mathbf{x}_0), \mathbf{v} \rangle / 2$ 
3:  $t = 0$ 
4: while  $\Phi_t > \varepsilon_{\text{tol}}$  and  $f(\mathbf{x}_t) - \Phi_t < \hat{f}$  do
   ▷ Near-optimal or pruned by the bound
5:    $a_t \leftarrow \operatorname{argmax}_{\mathbf{v} \in \mathcal{A}_t} \langle \nabla f(\mathbf{x}_t), \mathbf{v} \rangle$  ▷ away vertex
6:    $s_t \leftarrow \operatorname{argmin}_{\mathbf{v} \in \mathcal{A}_t} \langle \nabla f(\mathbf{x}_t), \mathbf{v} \rangle$  ▷ local forward vertex
7:   if  $\langle \nabla f(\mathbf{x}_t), a_t - s_t \rangle \geq \Phi_t$  then
8:      $d_t \leftarrow a_t - s_t$ 
9:      $\gamma_{\max} \leftarrow \operatorname{weight\_of}(\mathcal{A}_t, a_t)$ 
10:     $\gamma_t \leftarrow \operatorname{argmin} \gamma \in [0, \gamma_{\max}] f(x - \gamma d_t)$ 
11:     $\mathbf{x}_{t+1} \leftarrow \mathbf{x}_t - \gamma_t d_t$ 
12:     $\Phi_{t+1} \leftarrow \Phi_t$ 
13:    if  $\gamma_t < \gamma_{\max}$  then ▷ descent step
14:       $\mathcal{A}_{t+1} \leftarrow \mathcal{A}_t$ 
15:    else ▷ drop step
16:       $\mathcal{A}_{t+1} \leftarrow \mathcal{A}_t \setminus \{a_t\}$ 
17:       $S_{t+1} \leftarrow S_t \cup \{a_t\}$ 
18:    end if
19:  else
20:     $s_t \leftarrow \operatorname{argmin}_{\mathbf{v} \in S_t} \langle \nabla f(\mathbf{x}_t), \mathbf{v} \rangle$  ▷ forward vertex from dropped vertices
21:    if  $\langle \nabla f(\mathbf{x}_t), a_t - s_t \rangle \geq \Phi_t$  then
22:       $\mathcal{A}_{t+1} \leftarrow \mathcal{A}_t \cup \{s_t\}$ 
23:       $S_{t+1} \leftarrow S_t \setminus \{s_t\}$ 
24:      descent or drop step
25:    else
26:       $w_t \leftarrow \operatorname{argmin}_{\mathbf{v} \in P} \langle \nabla f(\mathbf{x}_t), \mathbf{v} \rangle$  ▷ global LMO
27:      if  $\langle \nabla f(\mathbf{x}_t), \mathbf{x}_t - w_t \rangle \geq \Phi_t / K$  then
28:         $d_t = \mathbf{x}_t - w_t$ 
29:         $\gamma_t \leftarrow \operatorname{argmin}_{\gamma \in [0, 1]} f(x - \gamma d_t)$ 
30:         $\mathbf{x}_{t+1} \leftarrow \mathbf{x}_t - \gamma_t d_t$ 
31:         $\Phi_{t+1} \leftarrow \Phi_t$ 
32:         $\mathcal{A}_{t+1} \leftarrow \mathcal{A}_t \cup \{w_t\}$ 
33:      else
34:         $\mathbf{x}_{t+1} \leftarrow \mathbf{x}_t$ 
35:         $\Phi_{t+1} \leftarrow \Phi_t / 2$ 
36:         $\mathcal{A}_{t+1} \leftarrow \mathcal{A}_t$ 
37:      end if
38:    end if
39:  end if
40:   $t \leftarrow t + 1$ 
41: end while

```

Proof. Given the iterate $\mathbf{x}^{(t)}$, we start from the strong convexity property:

$$\langle \nabla f(\mathbf{x}^{(t)}), \mathbf{x} - \mathbf{x}^{(t)} \rangle + \frac{\mu}{2} \|\mathbf{x} - \mathbf{x}^{(t)}\|^2 \leq f(\mathbf{x}) - f(\mathbf{x}^{(t)}) \quad \forall \mathbf{x} \in \mathcal{X}.$$

Taking the minimum over all solutions $\mathbf{x} \in \mathcal{X}_M$, we obtain:

$$\begin{aligned} \min_{\mathbf{x} \in \mathcal{X}_M} f(\mathbf{x}) - f(\mathbf{x}^{(t)}) &\geq \min_{\mathbf{x} \in \mathcal{X}_M} \mathbf{x}_j \nabla f(\mathbf{x}^{(t)})_j + \sum_{k \neq j} \nabla f(\mathbf{x}^{(t)})_k (\mathbf{x} - \mathbf{x}^{(t)})_k + \frac{\mu}{2} \|\mathbf{x} - \mathbf{x}^{(t)}\|^2 \\ &\geq \min_{\mathbf{x} \in \mathcal{X}_M} \mathbf{x}_j \nabla f(\mathbf{x}^{(t)})_j + \min_{\mathbf{x} \in \mathcal{X}_M} \sum_{k \neq j} \nabla f(\mathbf{x}^{(t)})_k (\mathbf{x} - \mathbf{x}^{(t)})_k + \min_{\mathbf{x} \in \mathcal{X}_M} \frac{\mu}{2} \|\mathbf{x} - \mathbf{x}^{(t)}\|^2 \\ &\geq M \nabla f(\mathbf{x}^{(t)})_j - g(\mathbf{x}^{(t)}) + \frac{\mu}{2} M^2, \end{aligned}$$

since the optimum in \mathcal{X}_M has at least the j -th variable at distance M from $\mathbf{x}^{(t)}$. This results in the following modification of inequality (3):

$$UB - f(\mathbf{x}^{(t)}) \geq M \nabla f(\mathbf{x}^{(t)})_j - g(\mathbf{x}^{(t)}) + \frac{\mu}{2} M^2. \quad (7)$$

Therefore, if (7) does not hold, i.e.:

$$M \nabla f(\mathbf{x}^{(t)})_j > UB - f(\mathbf{x}^{(t)}) + g(\mathbf{x}^{(t)}) - \frac{\mu}{2} M^2,$$

we can deduce $\mathbf{x}_j \leq \mathbf{l}_j + M - 1$. \square

Appendix C. Additional experiments

We add two sets of instances to complement our results.

Grouped sparse regression. In addition to cardinality, our framework can represent richer generic constraints in regression models, for example adding group sparsity, where variables are partitioned into subsets and only a few of those subsets can be in the support of the predictor. This results in a cardinality-constrained version of the *grouped lasso* model (Lounici et al., 2011; Friedman et al., 2010). Similarly to sparse regression, our framework can tackle grouped regression for all differentiable convex losses including Poisson, logistic, and linear regression.

MIPLIB instance. Our framework can process standard instance formats out of the box through the MathOptInterface library (Legat et al., 2022). We use some (bounded) instances from the MIPLIB 2017 (Gleixner et al., 2021) and, as a simple experiment, we compute vertices for random directions and then minimize the sum of squared distances to these vertices, therefore promoting interior integral solutions. The instances used are pg5_34, neos5 and 22433. They are solved both with our implementation Boscia and a pure Branch-And-Bound framework using Ipopt as the NLP solver. The computations in Figures 29, 28 and 27 illustrate that while the node evaluation is slower due to the MIP solver, we get feasible integral solutions and therefore valid upper bounds for free starting from the root node. Additionally, the convex hull of integer points is tighter than the relaxed feasible region. Hence, Ipopt's lower bound is much lower than the incumbent and while the node evaluation is much faster with Ipopt, many more nodes have to be evaluated. For better comparability, we provide BnB Ipopt with the best solution found in Boscia as an initial upper bound.

Figure 13 shows the primal-dual convergence for an integer regression problem with cardinality constraints. For all instances, the optimal primal solution is found early in the process, typically at the root node thanks to the optimization performed over the integer hull, the following nodes are used only to prove (near-)optimality.

Figure 12 shows the effect of tuning the FW gap tolerance at each node with the layer-dependent error.

In Figure 11, we test the effect of the lazification and warm-starting techniques added to BPCG, the root node requires the most LMO calls of all layers and populates the active and shadow sets. Depending on the instances, the cardinality of the active set and shadow sets evolve differently, depending on whether the last layers of nodes densify or sparsify the solution.

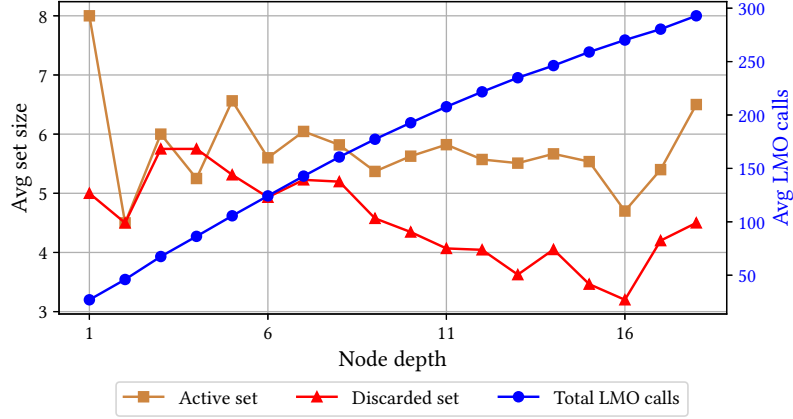


Figure 11: Average cardinality of the active & shadow sets and number of LMO calls over nodes at each depth level of the tree for the permutation matrices example with $n, k = 3$. The number of vertices in the active and shadow sets increases moderately while the number of LMO calls drops quickly after the root node.

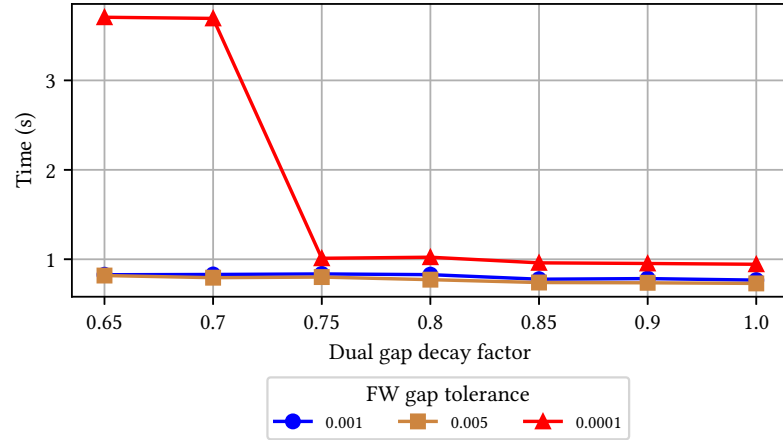


Figure 12: Effect of the FW gap tolerance parameters on the total solving time on integer sparse regression. Solving the subproblems with a too high accuracy is much costlier for the runtime. Furthermore, a lower decay rate, which implies nodes lower in the tree are solved with an accuracy that does not increase sharply with the depth, seems to accelerate the solving process.

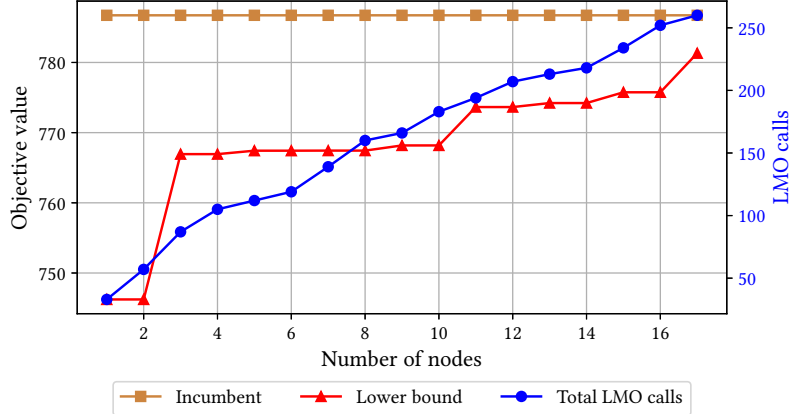


Figure 13: Convergence plot for an integer regression example in dimension 40 with a cardinality constraint on the support of the predictor. On most instances, the primal optimum is found at the root node, the remaining nodes are spent proving optimality within the specified relative gap tolerance of 1%.

Branching strategies

We present additional results comparing the strong and hybrid branching strategies to most infeasible (most fractional) branching. Strong branching is not beneficial for all problems. In particular, strong and hybrid branching provides a strong advantage for the dual bound progress when some branching decisions significantly tighten the problem. In some cases such as the mixed-binary quadratic problem shown in Figure 14, the most infeasible branching strategy is less efficient both against the number of nodes and time despite being a much cheaper variable selection heuristic.

Figure 16 shows the evolution of the dual bound when using different maximum depth levels for hybrid strong branching. The most expensive strategies using strong branching further down the tree are favorable even against time. This opens a range of algorithmic questions on adaptive transitions from strong branching to less expensive heuristics.

Figure 17 shows the evolution of the number of LMO calls and cardinality of the average number of active and shadow set for each node depth. We systematically observe a decrease in the number of LMO calls across layers thanks to warm starts and lazification. For some instances, the active set cardinality drops in the last layer, i.e. final solutions are sparser than the ones from previous layers. In some other instances, the leaf nodes produce denser solutions once all integers are fixed.

Figure 19 shows the primal-dual convergence on the sparse Poisson regression example in dimension 70. Unlike most other examples we covered, the gap is closed by a sharp drop of the incumbent value and not by an increase of the dual bound. This suggests a potential for improvement from designing and adding more advanced objective-aware heuristics (e.g. a nonlinear feasibility pump) or adjusting the heuristic collection from the MIP solver.

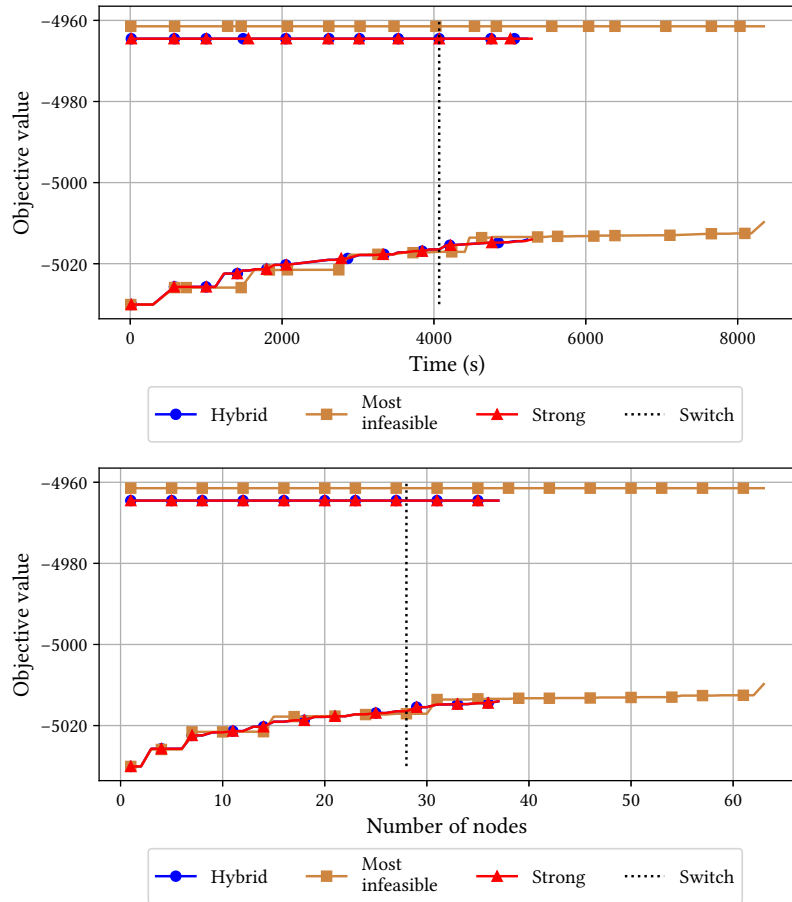


Figure 14: Primal-dual bound convergence for a low-dimensional quadratic mixed-binary problem (12) with a high inner dimension (500) taken from [Hunkenschröder et al. \(2022\)](#).

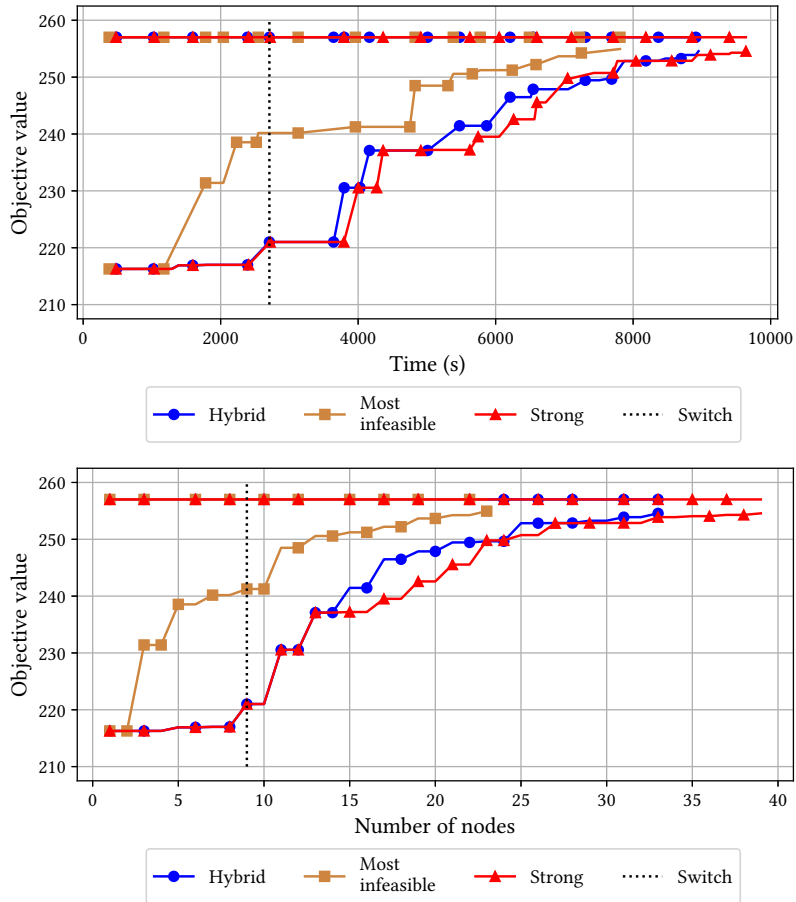


Figure 15: Dual bound convergence for grouped sparse regression against time and number of nodes. The switching limit corresponds to the last node where the hybrid branching applies strong branching.

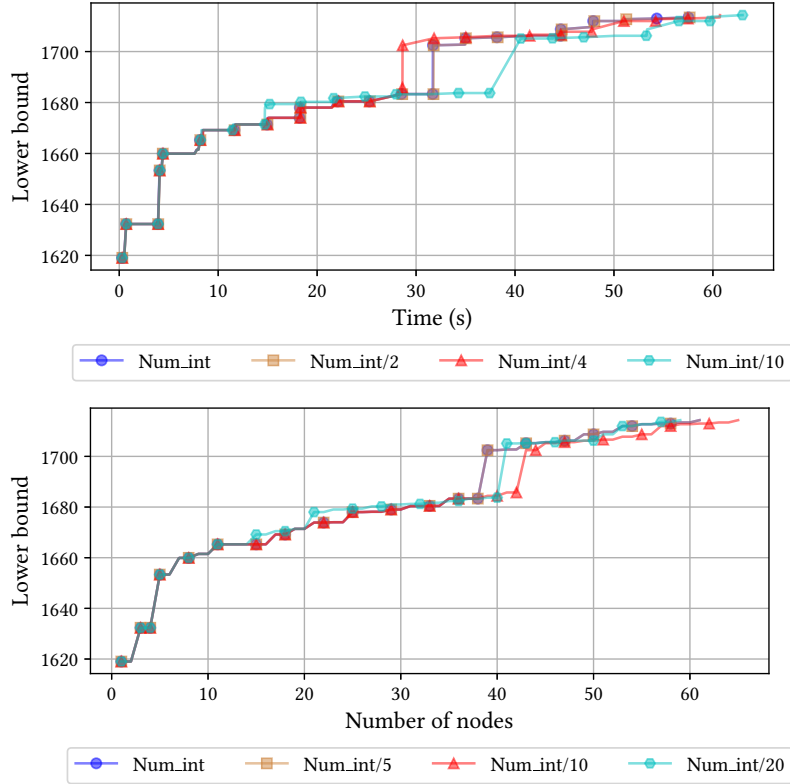


Figure 16: Depth adjustment for hybrid branching i.e. maximum depth up to which partial strong branching is applied before switching to most fractional branching on an integer sparse regression example. `Num_int` corresponds to a maximum depth equal to the number of integer variables. Since this instance has general integer variables and not only binary variables, this is not the maximum depth of the tree. The lowest numbers correspond to fewer strong branching calls. The maximum number of FW iterations was 10 and the gap tolerance 10^{-3} .

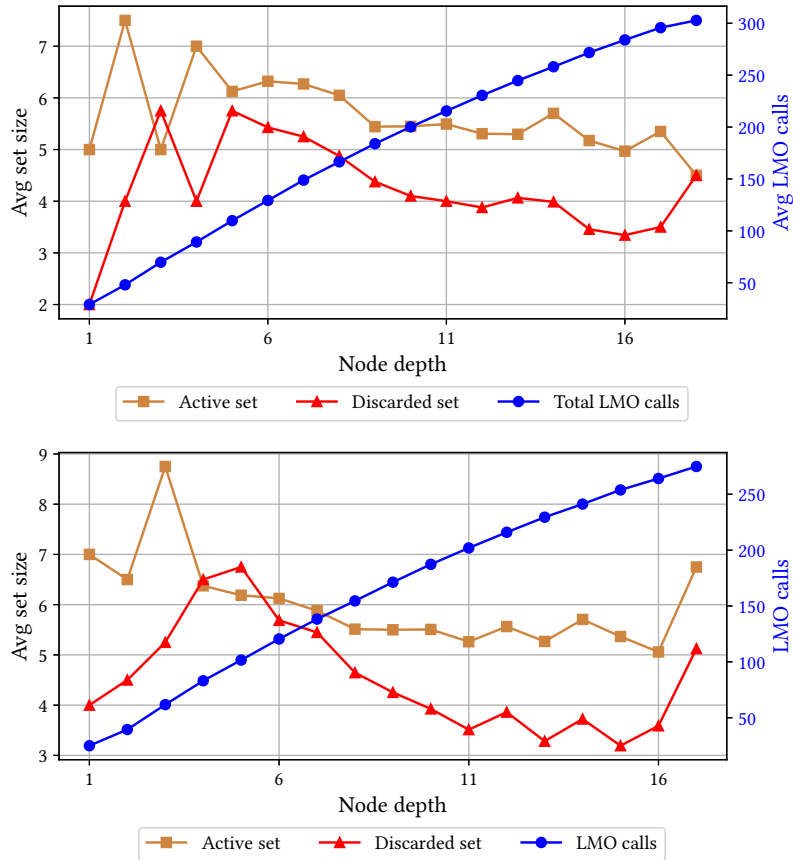


Figure 17: Evolution of the LMO call, active and shadow set cardinalities for the permutation matrices example.

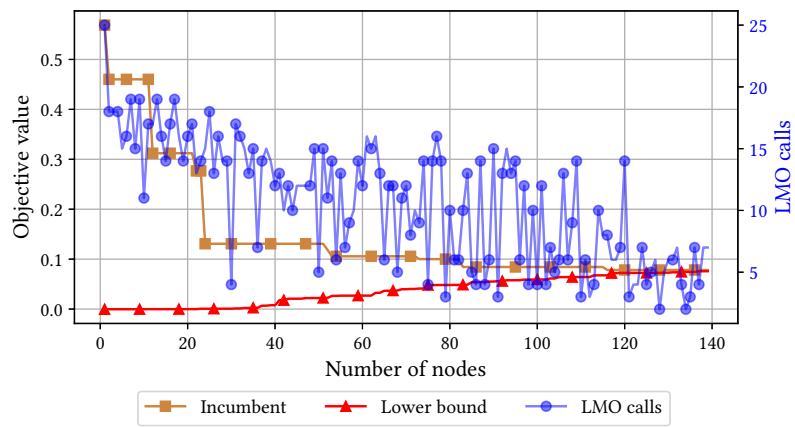


Figure 18: Primal-dual convergence on the permutation matrices example. The number of LMO calls is displayed for each node and decreases with the layers.

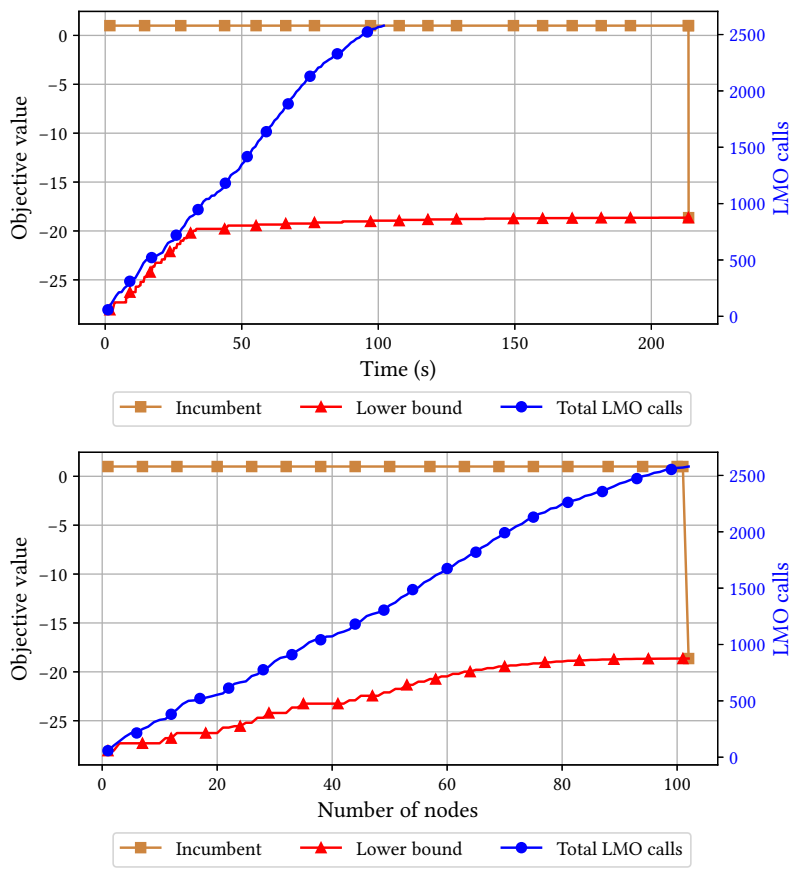
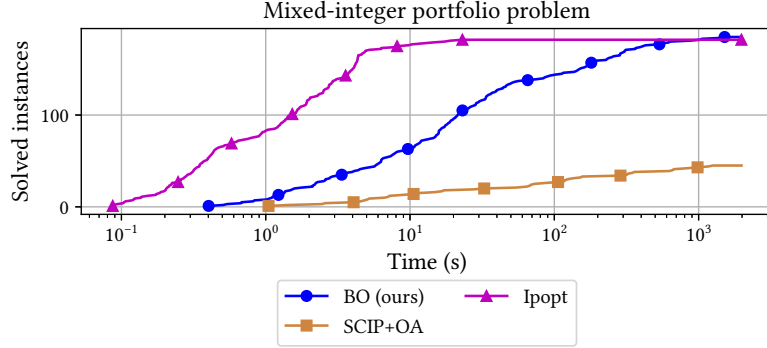
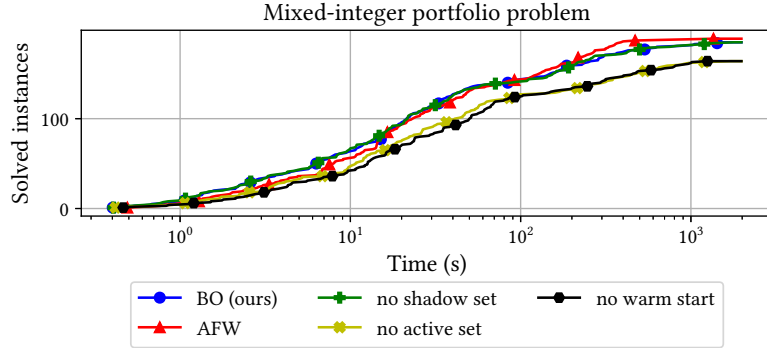


Figure 19: Primal-dual convergence on the sparse Poisson regression example.

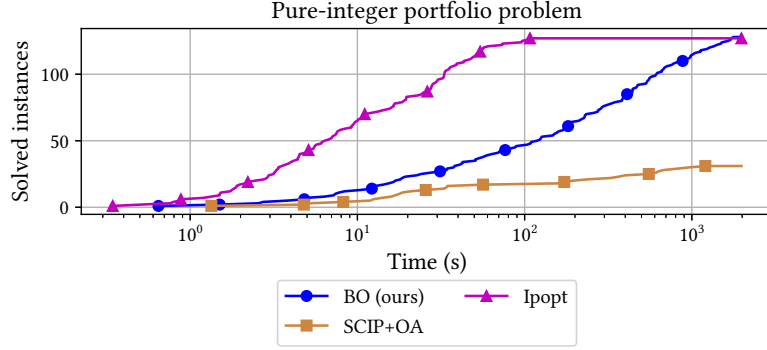


(a) The number of optimally solved mixed-integer portfolio instances within the time limit of 1800 seconds and the required time by our solver Boscia, outer approximation with SCIP and the interior point solver Ipopt. An instance is considered optimal if the objective value of the solution is close to the minimal value found by any of the three solvers with an absolute tolerance of 1e-4 and a relative tolerance of 1e-2.

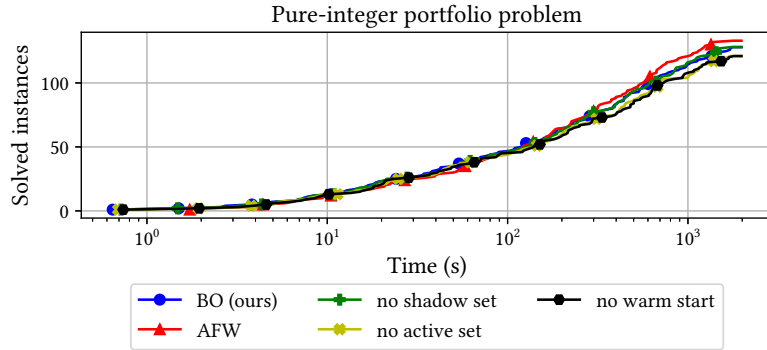


(b) The number of optimally solved mixed-integer portfolio instances and the required time by different warm-start and FW methods within the time limit of 1800 seconds. Boscia uses the pairwise conditional gradient and warm-start of the active set and shadow set. AFW uses the Away-step FW and warm start.

Figure 20: The number of optimally solved mixed-integer portfolio instances and the required time by different solvers and different warm-start methods.

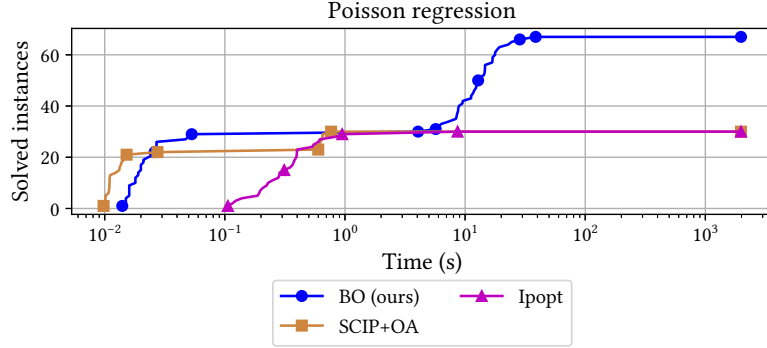


(a) The number of optimally solved pure-integer portfolio instances within the time limit of 1800 seconds and the required time by our solver Boscia, outer approximation with SCIP and the interior point solver Ipopt. An instance is considered optimal if the objective value of the solution is close to the minimal value found by any of the three solvers with an absolute tolerance of 1e-4 and a relative tolerance of 1e-2.

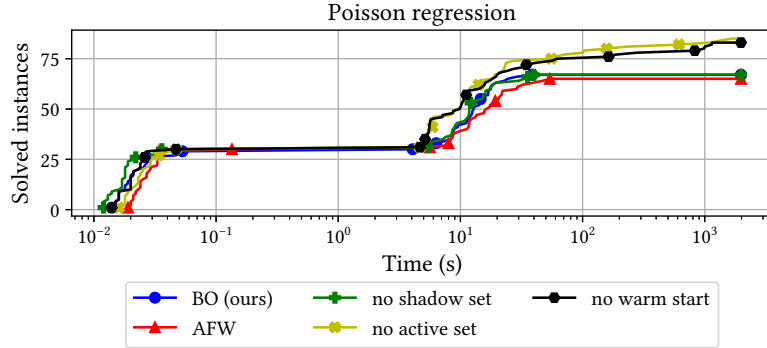


(b) The number of optimally solved pure-integer portfolio instances and the required time by different warm-start and FW methods within the time limit of 1800 seconds. Boscia uses the pairwise conditional gradient and warm-start of the active set and shadow set. AFW uses the Away-step FW and warm start.

Figure 21: The number of optimally solved pure-integer portfolio instances and the required time by different solvers and different warm-start methods.

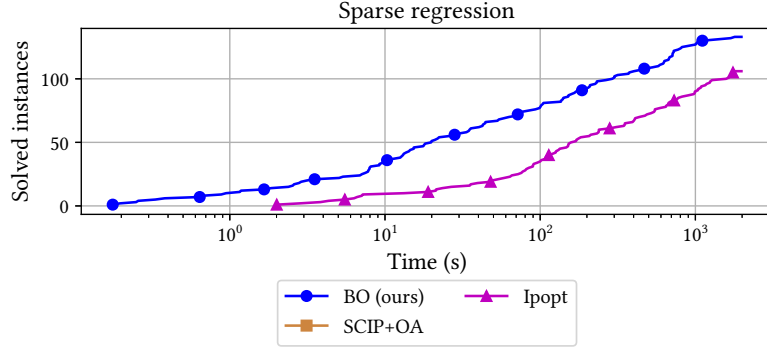


(a) The number of optimally solved Poisson regression instances within the time limit of 1800 seconds and the required time by our solver Boscia, outer approximation with SCIP and the interior point solver Ipopt. An instance is considered optimal if the objective value of the solution is close to the minimal value found by any of the three solvers with an absolute tolerance of $1e-4$ and a relative tolerance of $1e-2$.

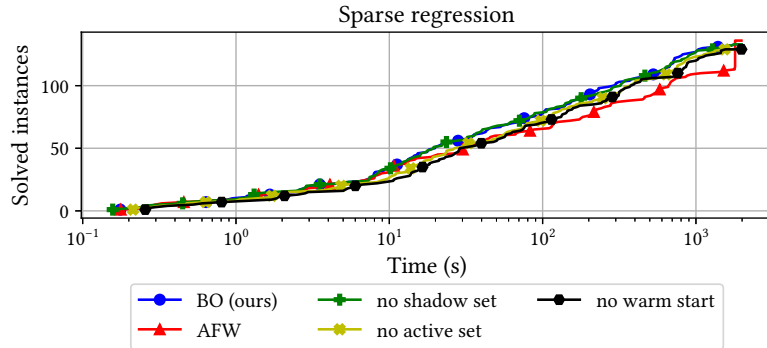


(b) The number of optimally solved Poisson regression instances and the required time by different warm-start and FW methods within the time limit of 1800 seconds. Boscia uses the pairwise conditional gradient and warm-start of the active set and shadow set. AFW uses the Away-step FW and warm start.

Figure 22: The number of optimally solved Poisson regression instances and the required time by different solvers and different warm-start methods.

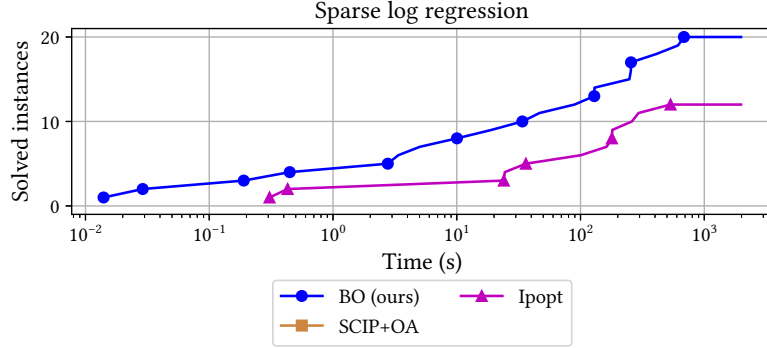


(a) The number of optimally solved sparse regression instances within the time limit of 1800 seconds and the required time by our solver Boscia, outer approximation with SCIP and the interior point solver Ipopt. An instance is considered optimal if the objective value of the solution is close to the minimal value found by any of the three solvers with an absolute tolerance of 1e-4 and a relative tolerance of 1e-2.

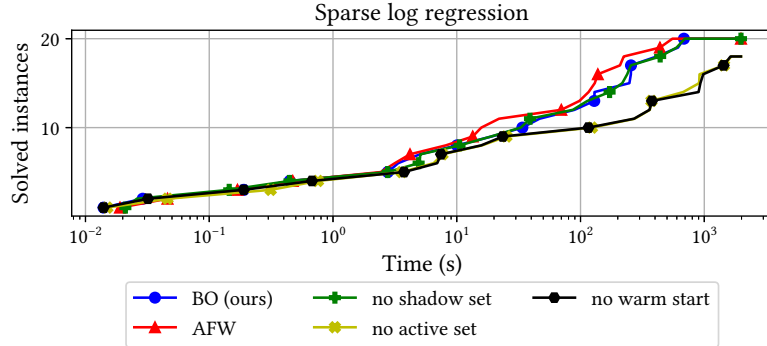


(b) The number of optimally solved sparse regression instances and the required time by different warm-start and FW methods within the time limit of 1800 seconds. Boscia uses the pairwise conditional gradient and warm-start of the active set and shadow set. AFW uses the Away-step FW and warm start.

Figure 23: The number of optimally solved sparse regression instances and the required time by different solvers and different warm-start methods.

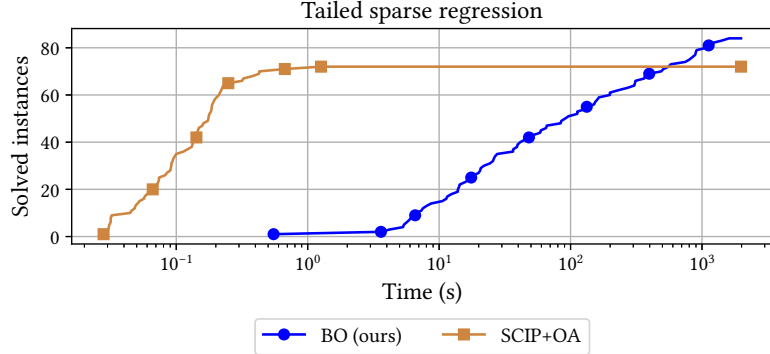


(a) The number of optimally solved sparse logistic regression instances within the time limit of 1800 seconds and the required time by our solver Boscia, outer approximation with SCIP and the interior point solver Ipopt. An instance is considered optimal if the objective value of the solution is close to the minimal value found by any of the three solvers with an absolute tolerance of $1e-4$ and a relative tolerance of $1e-2$.

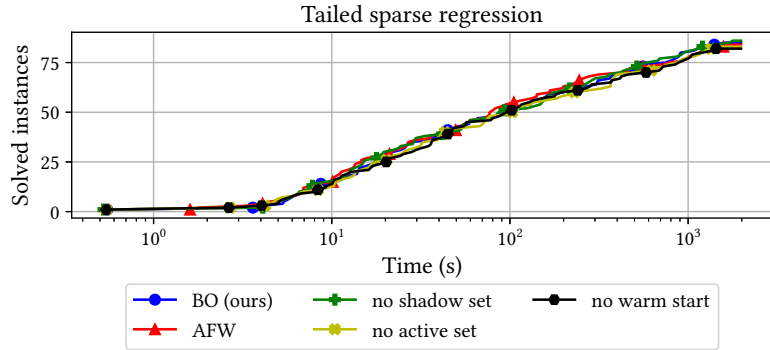


(b) The number of optimally solved sparse logistic regression instances and the required time by different warm-start and FW methods within the time limit of 1800 seconds. Boscia uses the pairwise conditional gradient and warm-start of the active set and shadow set. AFW uses the Away-step FW and warm start.

Figure 24: The number of optimally solved sparse logistic regression instances and the required time by different solvers and different warm-start methods.

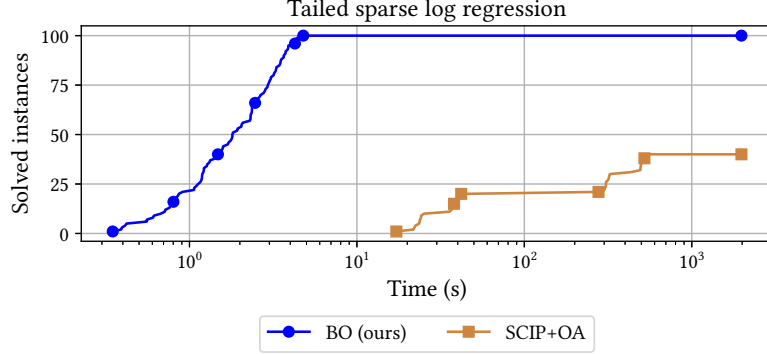


(a) The number of optimally solved two-tailed sparse regression instances within the time limit of 1800 seconds and the required time by our solver Boscia, outer approximation with SCIP and the interior point solver Ipopt. An instance is considered optimal if the objective value of the solution is close to the minimal value found by any of the three solvers with an absolute tolerance of $1e-4$ and a relative tolerance of $1e-2$.

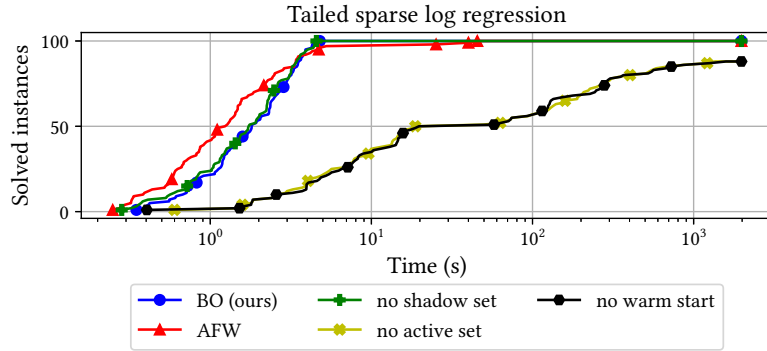


(b) The number of optimally solved two-tailed sparse regression instances and the required time by different warm-start and FW methods within the time limit of 1800 seconds. Boscia uses the pairwise conditional gradient and warm-start of the active set and shadow set. AFW uses the Away-step FW and warm start.

Figure 25: The number of optimally solved two-tailed sparse regression instances and the required time by different solvers and different warm-start methods.



(a) The number of optimally solved two-tailed sparse logistic regression instances within the time limit of 1800 seconds and the required time by our solver Boscia, outer approximation with SCIP and the interior point solver Ipopt. An instance is considered optimal if the objective value of the solution is close to the minimal value found by any of the three solvers with an absolute tolerance of $1e-4$ and a relative tolerance of $1e-2$.



(b) The number of optimally solved two-tailed sparse logistic regression instances and the required time by different warm-start and FW methods within the time limit of 1800 seconds. Boscia uses the pairwise conditional gradient and warm-start of the active set and shadow set. AFW uses the Away-step FW and warm start.

Figure 26: The number of optimally solved two-tailed sparse logistic regression instances and the required time by different solvers and different warm-start methods.

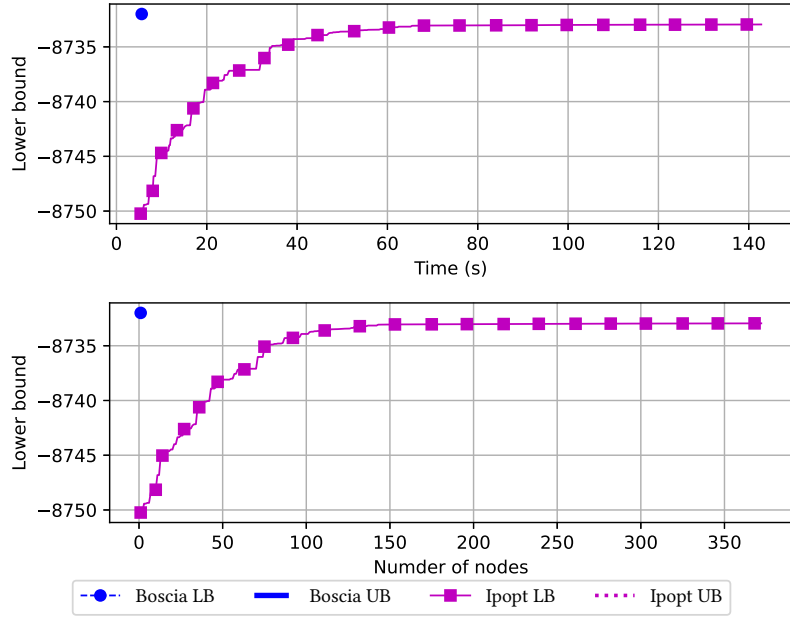


Figure 27: Primal-dual convergence comparison between Boscia and Ipopt for the MIP 22433 example. Ipopt has not found an integral leaf hence its upper bound is infinity for the entire run.

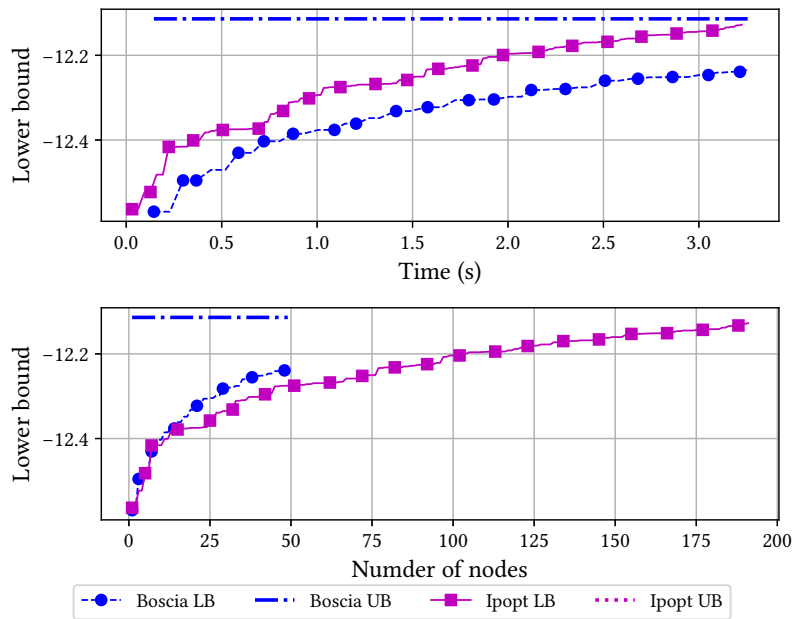


Figure 28: Primal-dual convergence comparison between Boscia and Ipopt for the MIP neos5 example.

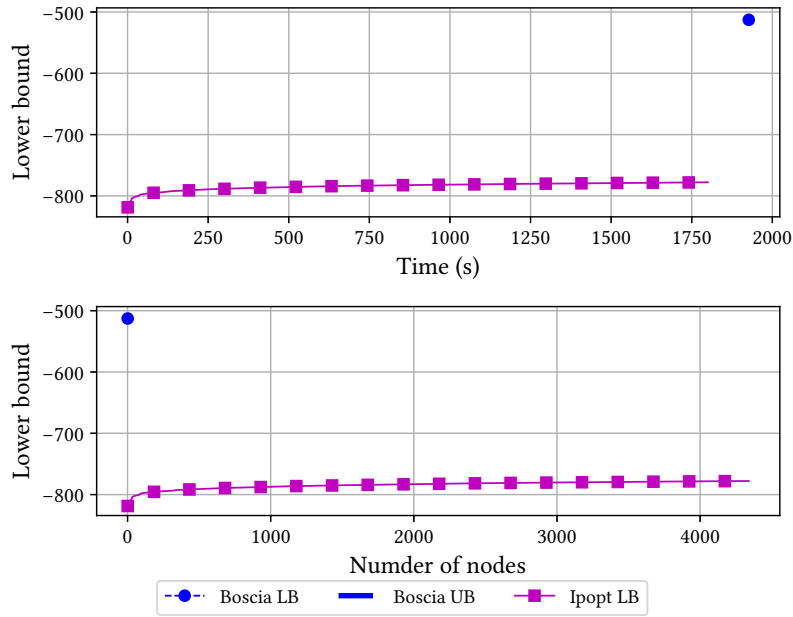


Figure 29: Primal-dual convergence comparison between Boscia and Ipopt for the MIP pg5_34 example. Ipopt has not found an integral leaf hence its upper bound is infinity for the entire run.

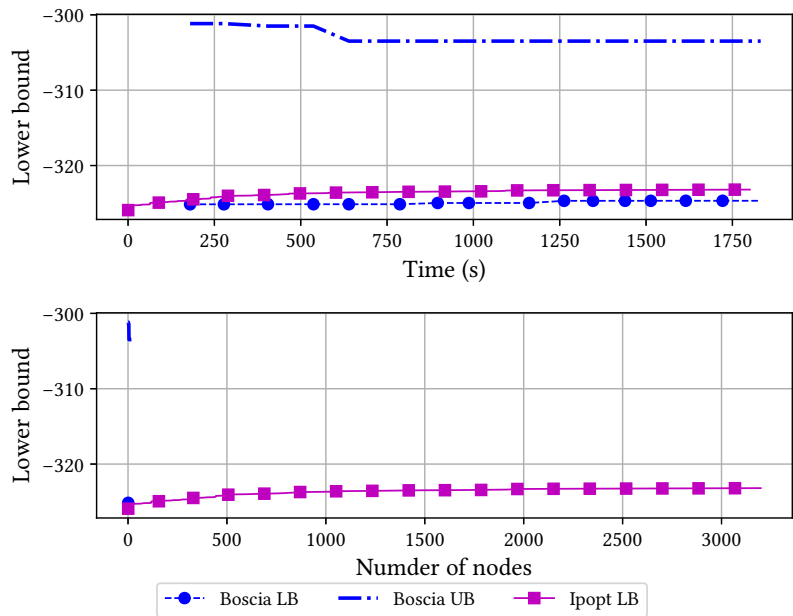


Figure 30: Primal-dual convergence comparison between Boscia and Ipopt for the MIP ran14x18-disj-8 example. Ipopt has not found an integral leaf hence its upper bound is infinity for the entire run.

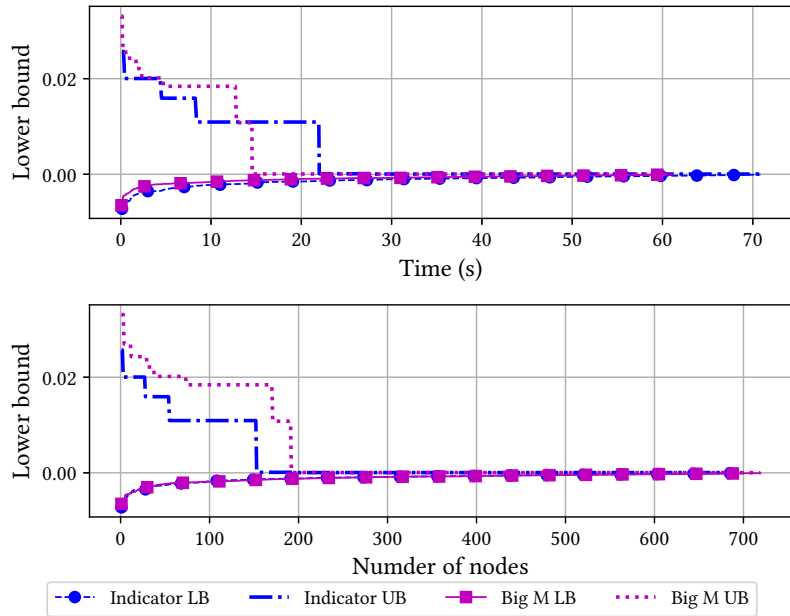


Figure 31: Primal-dual convergence comparison between using big-M and indicator formulation for the lasso problem.

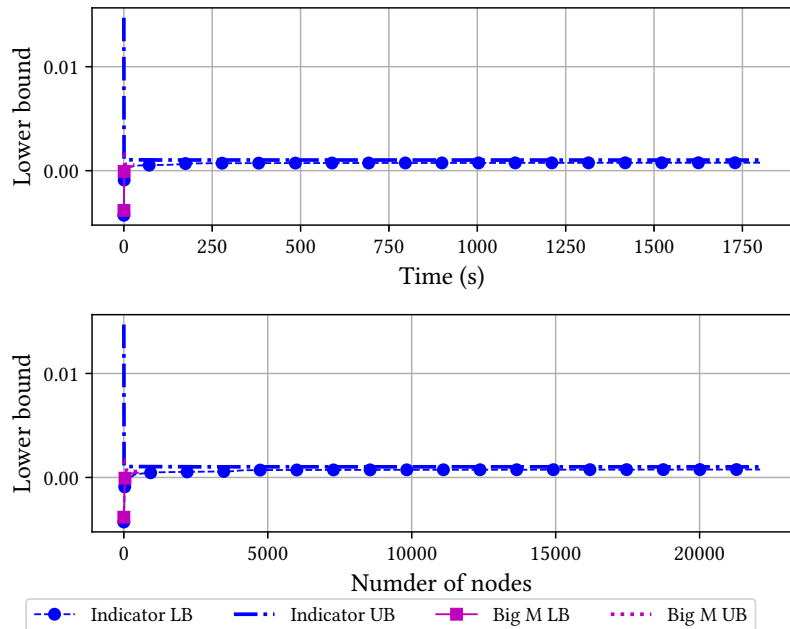


Figure 32: Primal-dual convergence comparison between using big-M and indicator formulation for the sparse regression problem.

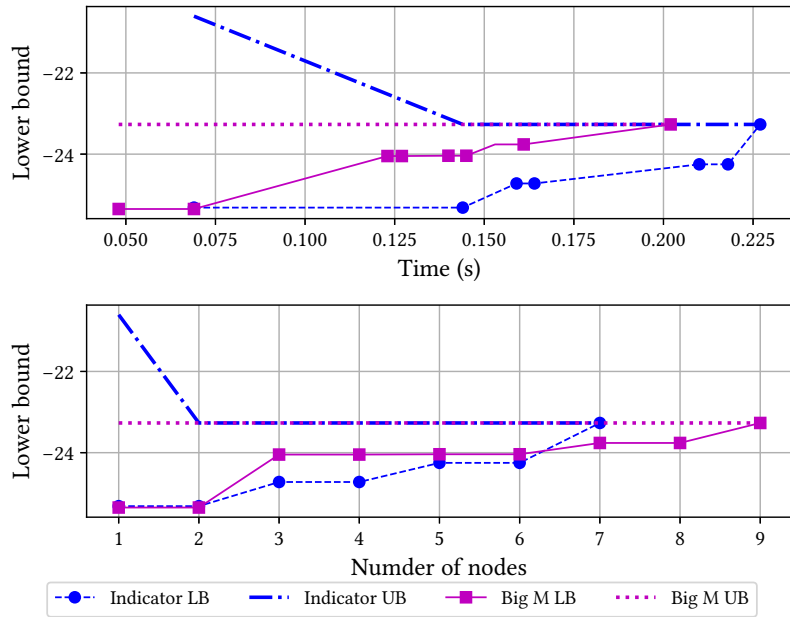


Figure 33: Primal-dual convergence comparison between using big-M and indicator formulation for the Poisson sparse regression problem.

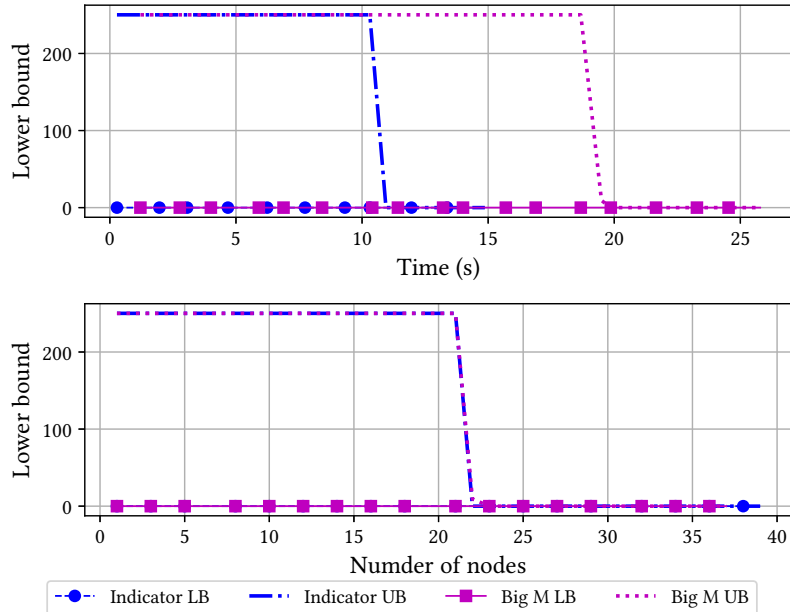


Figure 34: Primal-dual convergence comparison between using big-M and indicator formulation for the integer sparse regression problem.

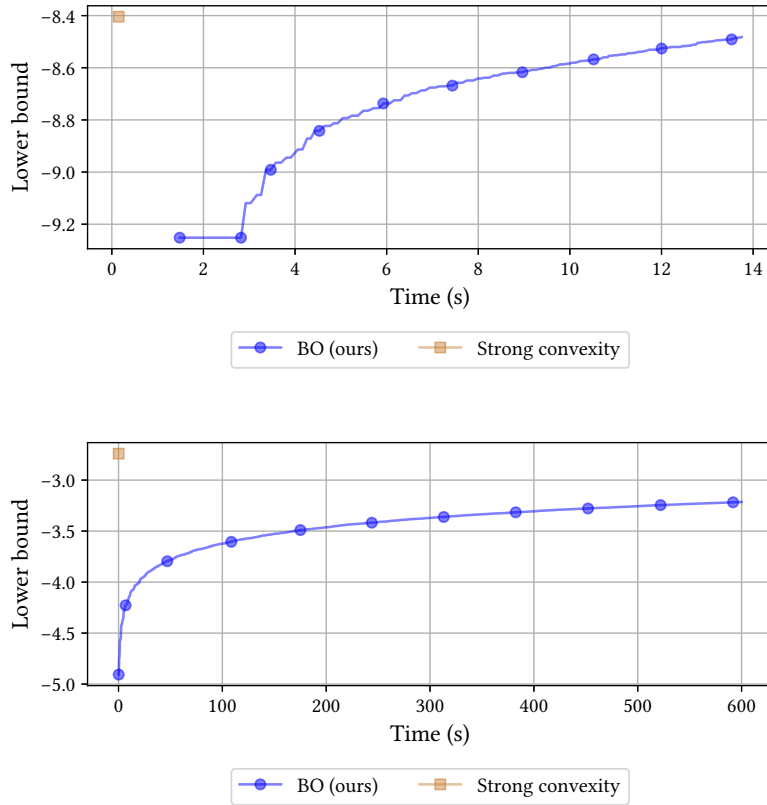


Figure 35: Dual bound convergence comparison between Boscia with and without exploiting strong convexity on the MIP neos5 example for different objective functions.

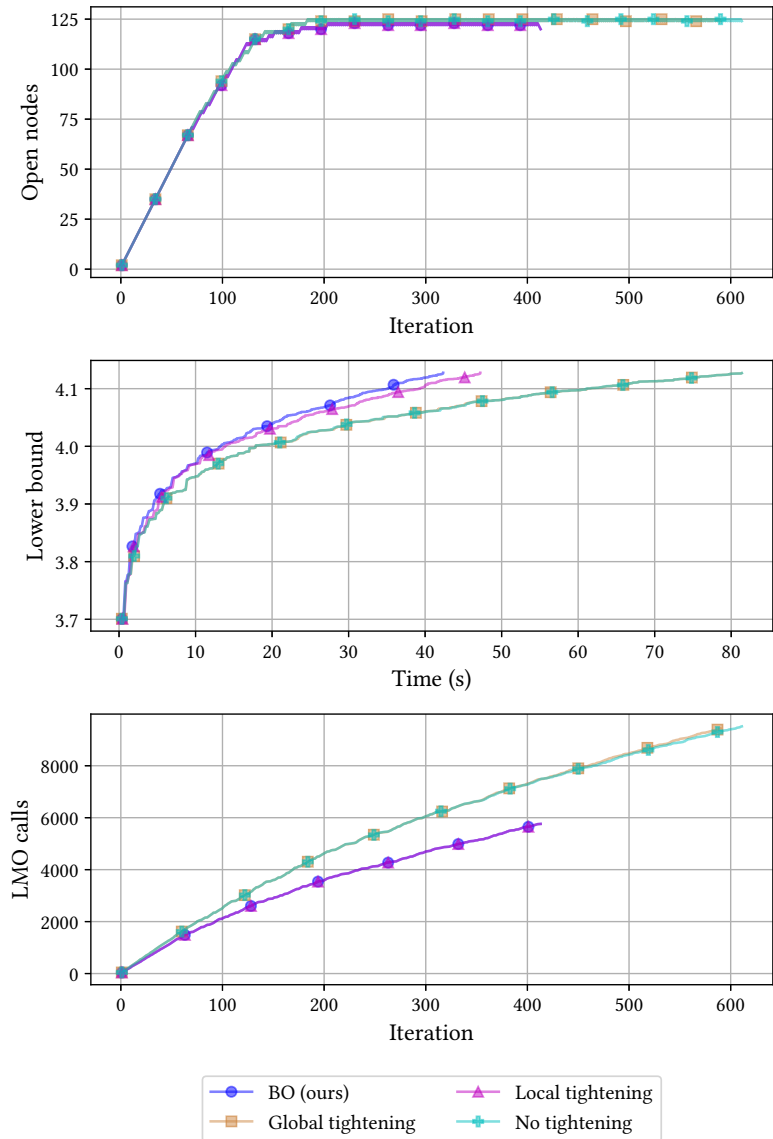


Figure 36: Comparison of the different tightening strategies on the sparse regression problem. We compare no tightening, only local tightening, only global tightening and Boscia which allows global and local tightening. We show the number of open nodes at each iteration, the lower bound convergence and the accumulated number of LMO calls at each iteration.

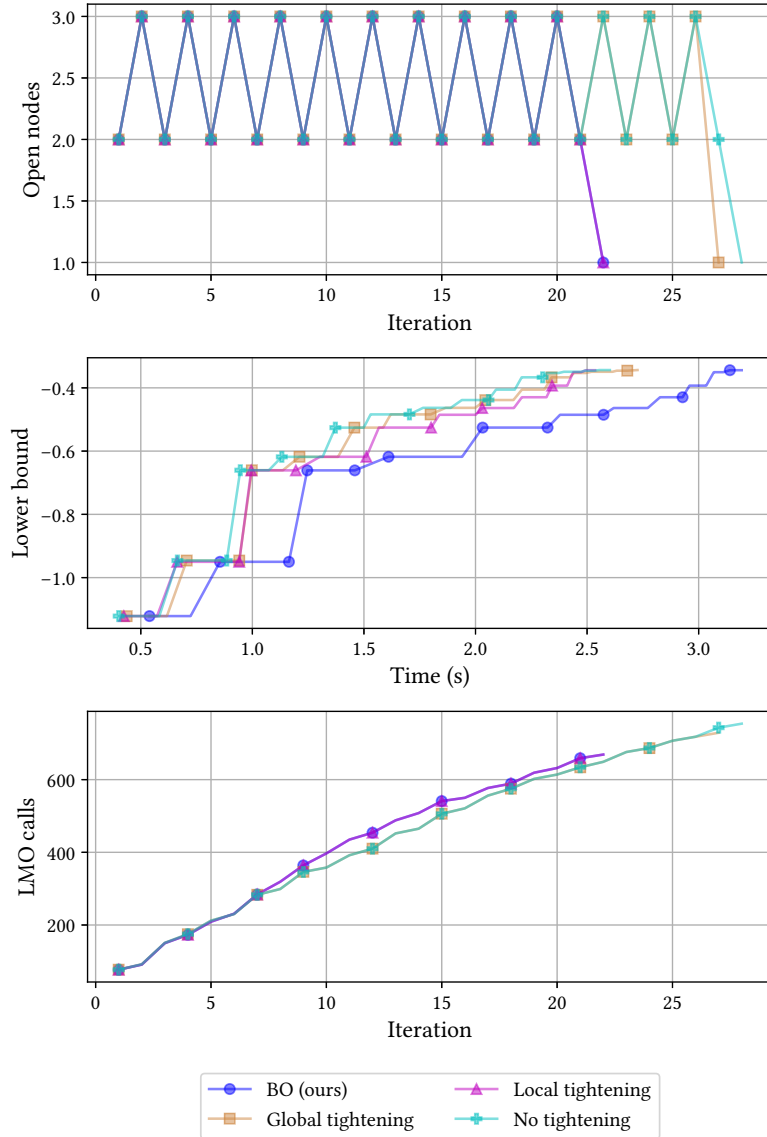


Figure 37: Comparison of the different tightening strategies on the mixed integer portfolio problem. We compare no tightening, only local tightening, only global tightening and Boscia which allows global and local tightening. We show the number of open nodes at each iteration, the lower bound convergence and the accumulated number of LMO calls at each iteration.

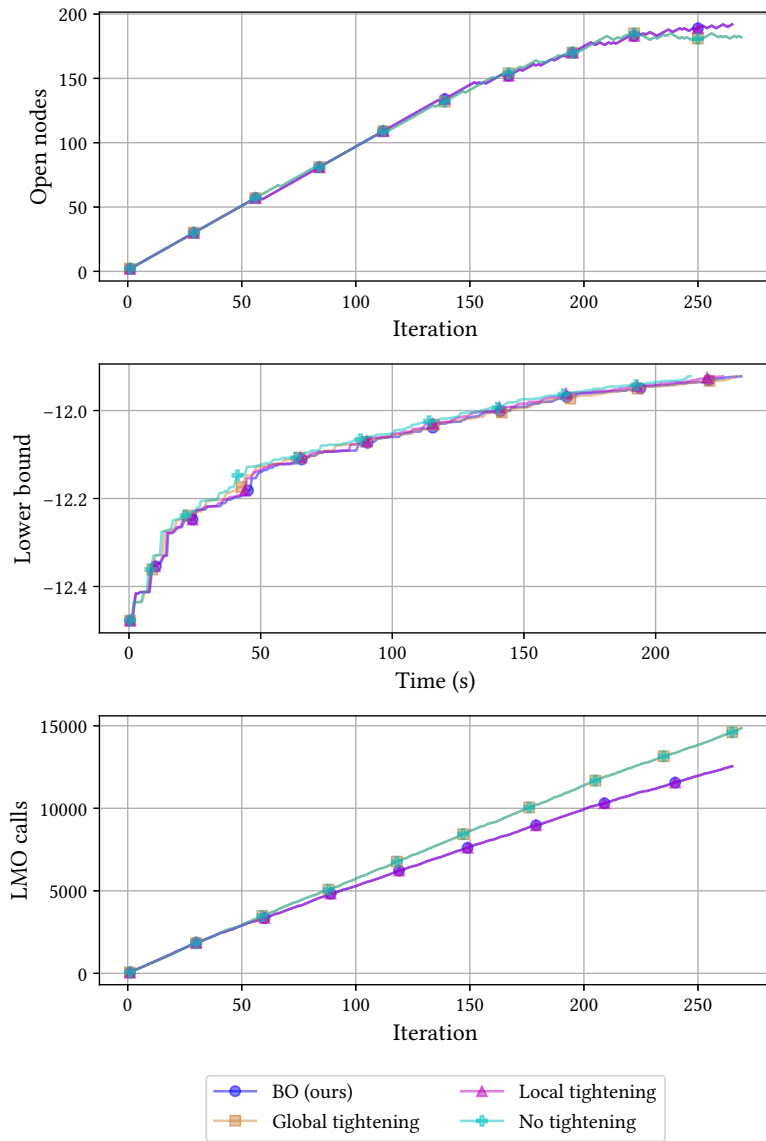


Figure 38: Comparison of the different tightening strategies on the integer portfolio problem. We compare no tightening, only local tightening, only global tightening and Boscia which allows global and local tightening. We show the number of open nodes at each iteration, the lower bound convergence and the accumulated number of LMO calls at each iteration.

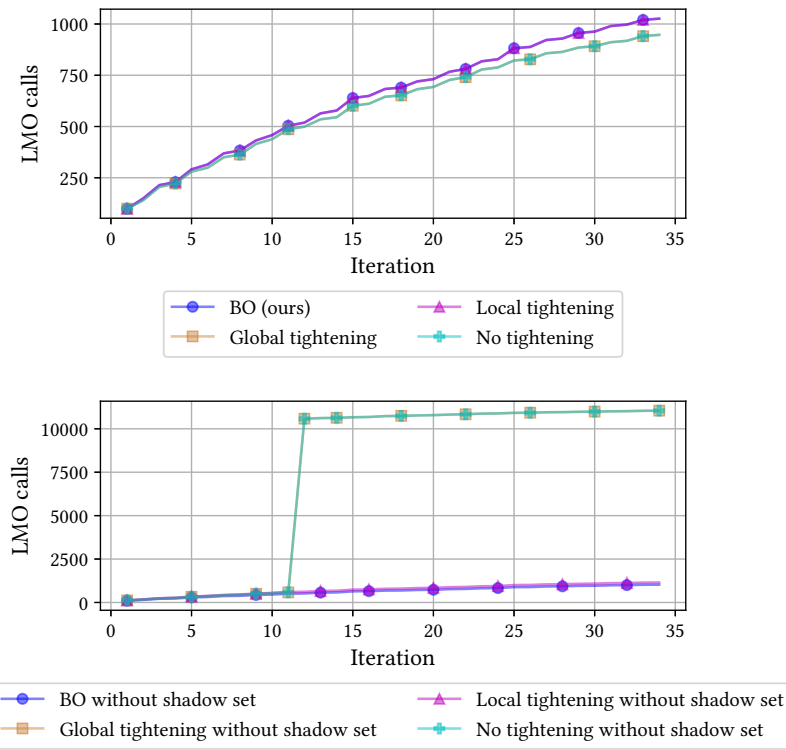


Figure 39: Comparison of the effect of tightening with and without warm start of the shadow set on the mixed integer portfolio problem with 20 continuous and 20 integer variables. Boscia applies local and global tightening.

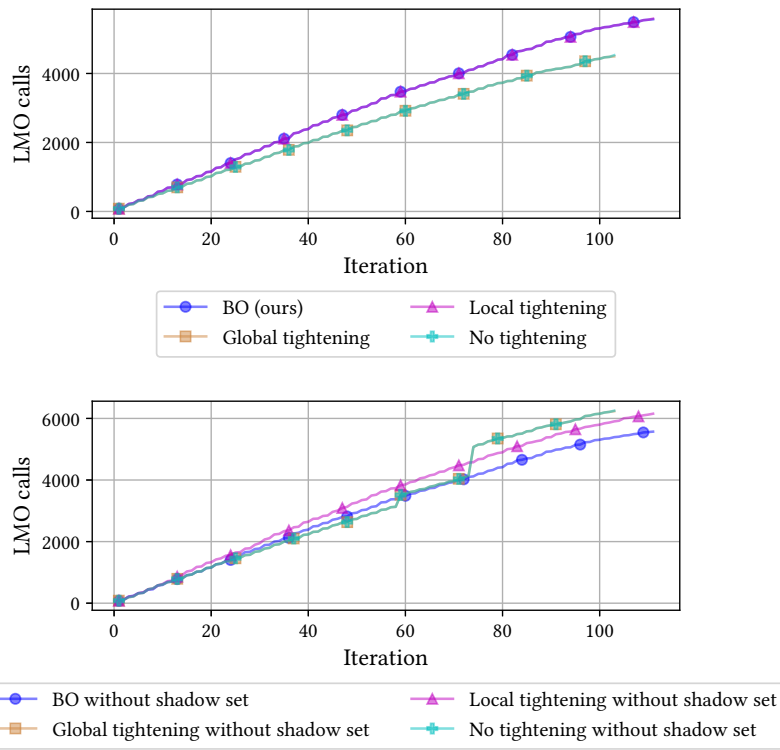


Figure 40: Comparison of the effect of tightening with and without warm start of the shadow set on the mixed integer portfolio problem with 25 continuous and 25 integer variables. Boscia applies local and global tightening.

Mixed Int Portfolio		Boscia		AFW		No Warm Start		No Active Set		No Shadow Set			
Dimension	Instances	Avg Time (s)	All-Solved (s)	# Solved	Avg Time (s)	All-Solved (s)	# Solved	Avg Time (s)	All-Solved (s)	# Solved	Avg Time (s)		
20	10	1	1	100%	1	1	100%	2	2	100%	1	1	100%
25	10	2	2	100%	3	3	100%	4	4	100%	3	2	100%
30	10	3	3	100%	4	4	100%	5	5	100%	5	3	100%
35	10	3	3	100%	4	4	100%	6	6	100%	6	3	100%
40	10	7	7	100%	12	12	100%	12	12	100%	12	7	100%
45	10	12	12	100%	18	18	100%	21	21	100%	20	12	100%
50	10	11	11	100%	12	12	100%	21	21	100%	18	11	100%
55	10	16	16	100%	19	19	100%	27	27	100%	21	13	100%
60	10	36	24	90%	36	23	90%	58	40	90%	54	36	90%
65	10	40	26	90%	35	23	90%	75	53	90%	62	43	90%
70	10	52	35	90%	47	31	90%	92	66	90%	91	66	90%
75	10	41	27	90%	44	29	90%	105	76	90%	93	67	90%
80	10	51	21	80%	90	43	80%	95	45	80%	84	39	80%
85	10	36	29	100%	33	26	100%	136	102	90%	112	82	90%
90	10	88	30	80%	81	29	80%	424	162	60%	373	140	70%
95	10	284	64	70%	194	58	70%	583	189	50%	674	252	50%
100	10	210	51	80%	198	49	80%	483	130	50%	496	137	50%
105	10	232	112	80%	153	97	90%	659	338	60%	668	345	60%
110	10	502	180	60%	373	151	70%	1174	619	40%	1269	751	40%
115	10	334	194	80%	260	172	90%	1141	445	40%	1125	375	30%
120	10	867	102	60%	448	115	70%	1629	665	10%	1575	472	10%

Table 1: The mixed-integer portfolio problem solved by using different warm-start and FW methods. Boscia uses the pairwise conditional gradient and warm-start of the active set and shadow set. AFW uses the Away-step FW and warm start. The dimension indicates the number of variables with $n/2$ integer and continuous variables. The average time is computed with the geometric mean. #Solved shows the absolute and relative number of instances solved in the time limit of 1800 seconds. All-solved is the average time used on instances that were solved by all different methods.

Mixed Int Portfolio		Boscia		SCIP+OA		Ipopt			
Dimension	Instances	Avg Time (s)	All-Optimal (s)	# Solved	Relative gap	Avg Time (s)	All-Optimal (s)	# Solved	Relative gap
20	10	1	1	100%	0.0	4	100%	0	0
25	10	2	2	100%	0.0	33	12	80%	0.0
30	10	3	3	100%	0.0	106	77	90%	0.0
35	10	3	4	100%	0.0	200	157	90%	0.0
40	10	7	5	100%	0.0	818	484	60%	10.0
45	10	12	3	100%	0.0	1271	316	20%	102.0
50	10	11	6	100%	0.0	1724	1171	10%	25560.0
55	10	16	-	100%	0.0	1800	-	0%	57940.0
60	10	36	-	90%	8.0	1800	-	0%	1.236866
65	10	40	-	90%	0.0	1800	-	0%	inf
70	10	52	-	90%	2.0	1800	-	0%	inf
75	10	41	-	90%	1.0	1800	-	0%	245975.0
80	10	51	-	80%	14.0	1800	-	0%	inf
85	10	36	-	100%	0.0	1800	-	0%	inf
90	10	88	-	80%	43.0	1800	-	0%	inf
95	10	284	-	70%	54.0	1800	-	0%	inf
100	10	210	-	80%	49.0	1800	-	0%	inf
105	10	232	-	80%	10371.0	1800	-	0%	inf
110	10	502	-	60%	3595.0	1800	-	0%	inf
115	10	334	-	80%	10348.0	1800	-	0%	inf
120	10	867	-	60%	321.0	1800	-	0%	inf

Table 2: Comparison of our solver Boscia, outer approximation with SCIP and the interior point solver Ipopt solving the mixed-integer portfolio problem. The dimension indicates the number of variables with $n/2$ integer and continuous variables. The average time is computed with the geometric mean. #Solved shows the absolute and relative number of instances solved in the time limit of 1800 seconds. An instance is considered optimal if the objective value of the solution is close to the minimal value found by any of the three solvers with an absolute tolerance of 1e-4 and a relative tolerance of 1e-2. All-optimal is the average time used on instances that were solved optimally by all solvers. “-” indicates that there is no instance solved by all different methods.

Integer Portfolio	Boscia			AFW			No Warm Start			No Active Set			No Shadow Set				
	Dimension	Instances	Avg Time (s)	All-Solved (s)	# Solved	Avg Time (s)	All-Solved (s)	# Solved	Avg Time (s)	All-Solved (s)	# Solved	Avg Time (s)	All-Solved (s)	# Solved			
20	10	5	5	10	100%	7	7	10	100%	6	6	10	100%	6	10	100%	
25	10	25	25	10	100%	31	31	10	100%	28	28	10	100%	28	10	100%	
30	10	40	40	10	100%	46	46	10	100%	43	43	10	100%	45	10	100%	
35	10	45	45	10	100%	58	58	10	100%	49	49	10	100%	46	10	100%	
40	10	205	161	9	90%	219	173	9	90%	215	170	9	90%	222	176	9	90%
45	10	253	203	9	90%	255	205	9	90%	288	234	9	90%	277	225	9	90%
50	10	185	144	9	90%	182	141	9	90%	218	172	9	90%	212	167	9	90%
55	10	267	165	8	80%	274	171	8	80%	304	195	8	80%	302	193	8	80%
60	10	582	274	6	60%	567	263	6	60%	649	329	6	60%	627	311	6	60%
65	10	502	365	8	80%	453	321	8	80%	620	475	8	80%	607	463	8	80%
70	10	1010	728	7	70%	875	638	7	70%	1142	843	6	60%	1170	877	6	60%
75	10	714	416	7	70%	585	340	8	80%	876	542	6	60%	833	506	7	70%
80	10	933	621	7	70%	770	488	7	70%	1090	789	7	70%	1038	719	6	60%
85	10	846	545	9	90%	646	433	9	90%	1017	695	6	60%	1021	700	6	60%
90	10	1083	505	5	50%	926	390	6	60%	1327	651	3	30%	1313	628	3	30%
95	10	1505	832	3	30%	1355	610	4	40%	1597	990	2	20%	1601	1003	2	20%
100	10	814	1	10%	917	2	1	10%	825	1	1	10%	820	1	1	10%	
105	10	1800	-	0	0%	1690	-	2	20%	1780	-	1	10%	1774	-	1	10%
110	10	1800	-	0	0%	1800	-	0	0%	1800	-	0	0%	1800	-	0	0%
115	10	1800	-	0	0%	1800	-	0	0%	1800	-	0	0%	1800	-	0	0%
120	10	1800	-	0	0%	1800	-	0	0%	1800	-	0	0%	1800	-	0	0%

Table 3: The pure integer portfolio problem solved by using different warm-start and FW methods. Boscia uses the pairwise conditional gradient and warm-start of the active set and shadow set. AFW uses the Away-step FW and warm start. The dimension indicates the number of variables with $n/2$ integer and continuous variables. The average time is computed with the geometric mean. # Solved shows the absolute and relative number of instances solved in the time limit of 1800 seconds. All-solved is the average time used on instances that where solved by all different methods. “-” indicates that there is no instance that all methods could solve.

Integer Portfolio	Boscia			SCIP+OA			Ipopt			Relative gap				
	Dimension	Instances	Avg Time (s)	Optimal (s)	# Solved	Relative gap	Ave Time (s)	Optimal (s)	All-Optimal (s)					
20	10	5	5	10	100%	1.0	10	10	100%	1.0	2	10	100%	10.0
25	10	25	23	10	100%	1.0	183	142	80%	1.0	3	10	100%	10.0
30	10	40	27	10	100%	1.0	266	165	70%	1.0	4	2	100%	10.0
35	10	45	46	10	100%	1.0	891	748	40%	1.0	5	4	100%	10.0
40	10	205	97	9	90%	1.0	1729	1574	10%	20.0	13	5	100%	9.0
45	10	253	53	9	90%	3.0	1663	1382	10%	38.0	12	3	100%	9.0
50	10	185	172	9	90%	9.0	1800	0	0%	50.0	10	10	100%	9.0
55	10	267	382	8	80%	59.0	1800	0	0%	34.0	20	11	9	90%
60	10	582	-	6	60%	92.0	1800	-	0%	179.0	48	-	9	90%
65	10	502	-	8	80%	83.0	1800	-	0%	40.0	41	-	9	90%
70	10	1010	-	7	70%	44.0	1800	-	0%	794.0	78	-	9	90%
75	10	714	-	7	70%	75.0	1800	-	0%	38.0	60	-	9	90%
80	10	933	-	7	70%	83.0	1800	-	0%	114.0	114	-	8	80%
85	10	846	-	9	90%	34.0	1800	-	0%	86.0	53	-	10	100%
90	10	1083	-	5	50%	66.0	1800	-	0%	348.0	132	-	8	80%
95	10	1505	-	3	30%	294.0	1800	-	0%	Inf	276	-	7	70%
100	10	814	-	1	10%	212.0	1800	-	0%	Inf	226	-	8	80%
105	10	1800	-	0	0%	356.0	1800	-	0%	Inf	77	-	10	100%
110	10	1800	-	0	0%	172.0	1800	-	0%	Inf	159	-	9	90%
115	10	1800	-	0	0%	143.0	1800	-	0%	Inf	180	-	9	90%
120	10	1800	-	0	0%	1511.0	1800	-	0%	Inf	257	-	8	80%

Table 4: Comparison of our solver Boscia, outer approximation with SCIP and the interior point solver Ipopt solving the pure integer portfolio problem. The dimension indicates the number of variables with $n/2$ integer and continuous variables. The average time is computed with the geometric mean. # Solved shows the absolute and relative number of instances solved in the time limit of 1800 seconds. An instance is considered optimal if the objective value of the solution is close to the minimal value found by any of the three solvers with an absolute tolerance of 1e-4 and a relative tolerance of 1e-2. All-Optimal is the average time used on instances that were solved optimally by all solvers. “-” indicates that there is no instance that could be optimally solved by all.

Poisson Regression			Boscia			AW			No Warm Start			No Active Set			No Shadow Set			
Dimension	Bound	ℓ_{inf}	Instances	Avg Time (s)	All-Solved (s)	# Solved	Avg Time (s)	All-Solved (s)	# Solved	Avg Time (s)	All-Solved (s)	# Solved	Avg Time (s)	All-Solved (s)	# Solved	Avg Time (s)	All-Solved (s)	# Solved
50	25	0.1	10	0	0	0	10	100%	0	0	10	100%	0	0	10	100%	0	0
70	35	0.1	10	0	0	0	10	100%	0	0	10	100%	0	0	10	100%	0	0
90	45	0.1	10	0	0	0	10	100%	0	0	10	100%	0	0	10	100%	0	0
50	25	5.0	2	8	8	2	100%	17	17	2	100%	7	7	2	100%	7	6	
70	35	1.0	10	413	17	3	30%	659	9	2	20%	374	62	6	60%	210	61	7
70	35	5.0	10	12	11	10	100%	15	15	10	100%	8	8	10	100%	7	7	10
70	35	10.0	2	10	10	2	100%	8	8	2	100%	5	5	2	100%	5	5	2
90	45	1.0	10	401	11	3	30%	631	10	2	20%	102	25	8	80%	100	13	8
90	45	5.0	10	14	14	10	100%	21	21	10	100%	8	8	10	100%	9	9	10
90	45	10.0	7	15	15	7	100%	15	15	7	100%	13	13	7	100%	12	12	7
90	45	10.0	7	15	15	7	100%	15	15	7	100%	13	13	7	100%	14	14	7

Table 5: Poisson regression solved by using different warm-start and FW methods. Boscia uses the pairwise conditional gradient and warm-start of the active set and shadow set. AFW uses the Away-step FW and warm start. The dimension indicates the number of variables, where Bound is the number of integer variables. The average time is computed with the geometric mean. # Solved shows the absolute and relative number of instances solved in the time limit of 1800 seconds. All-solved is the average time used on instances that were solved by all different methods.

Poisson Regression			Boscia			SCIP+OA			Ipopt								
Dimension	Bound	ℓ_{inf}	Instances	Avg Time (s)	All-Optimal (s)	# Solved	Relative gap	Avg Time (s)	All-Optimal (s)	# Solved	Relative gap	Avg Time (s)	All-Optimal (s)	# Solved	Relative gap		
50	25	0.1	10	0	100%	0	0	0	100%	0	0	0	100%	0	0	100%	0.0
70	35	0.1	10	0	100%	0	0	0	100%	0	0	0	100%	0	0	100%	0.0
90	45	0.1	10	0	100%	0	0	0	100%	0	0	0	100%	0	0	100%	0.0
50	25	5.0	2	8	-	2	100%	0.0	4	-	1	50%	Inf	1800	-	0	0%
70	35	1.0	10	413	-	3	30%	1.0	0	-	10	100%	217.0	1800	-	0	0%
70	35	5.0	10	12	-	10	100%	0.0	542	-	1	10%	Inf	1800	-	0	0%
70	35	10.0	2	10	-	2	100%	0.0	1800	-	0	0%	Inf	1800	-	0	0%
90	45	1.0	10	401	-	3	30%	2.0	2	-	6	60%	1650.0	1800	-	0	0%
90	45	5.0	10	14	-	10	100%	0.0	1800	-	0	0%	Inf	1800	-	0	0%
90	45	10.0	7	15	-	7	100%	0.0	1800	-	0	0%	Inf	1800	-	0	0%

Table 6: Comparison of our solver Boscia, outer approximation with SCIP and the interior point solver Ipopt. The dimension indicates the number of variables, where Bound is the number of integer variables. The average time is computed with the geometric mean. # Solved shows the absolute and relative number of instances solved in the time limit of 1800 seconds. An instance is considered optimal if the objective value of the solution is close to the minimal value found by any of the three solvers with an absolute tolerance of 1e-4 and a relative tolerance of 1e-2. All-Optimal is the average time used on instances that were solved optimally by all solvers. “-” indicates that there is no instance that could be optimally solved by all.

Sparse Regression			Boscia		AFW		No Warm Start			No Active Set			No Shadow Set				
Dimension	Bound	Instances	Avg Time (s)	All-Solved (s)	# Solved	Avg Time (s)	All-Solved (s)	# Solved	Avg Time (s)	All-Solved (s)	# Solved	Avg Time (s)	All-Solved (s)	# Solved			
75	3	10	2	2	10	100%	19	10	100%	4	10	100%	4	10	100%		
80	4	10	12	7	10	100%	16	9	100%	17	10	90%	14	8	90%		
85	4	10	9	5	9	90%	13	8	90%	14	8	90%	12	7	90%		
90	4	10	14	14	10	100%	32	10	100%	23	10	100%	20	20	100%		
95	4	10	11	11	10	100%	15	15	100%	20	20	100%	17	17	100%		
100	4	10	37	24	9	90%	155	118	100%	73	51	90%	54	37	90%		
105	5	10	74	52	9	90%	90	64	9	90%	65	9	90%	77	54	90%	
110	5	10	137	103	9	90%	168	129	9	90%	186	145	9	90%	154	118	90%
115	5	10	155	118	9	90%	186	145	9	90%	231	184	9	90%	192	150	90%
120	5	10	200	115	9	90%	199	115	9	90%	272	170	8	80%	237	143	80%
125	5	10	178	100	8	80%	217	128	8	80%	246	149	8	80%	264	163	80%
130	6	10	505	293	7	70%	695	462	7	70%	611	385	7	70%	588	364	70%
135	6	10	324	268	9	90%	290	237	9	90%	393	332	9	90%	355	296	90%
140	6	10	592	237	6	60%	749	382	6	60%	884	434	5	50%	896	446	50%
145	6	10	655	146	5	50%	624	133	5	50%	675	155	4	40%	651	142	40%
150	6	10	795	233	4	40%	760	220	6	60%	857	282	4	40%	881	302	40%

Table 7: Sparse regression problems solved by using different warm-start and FW methods. Boscia uses the pairwise conditional gradient and warm-start of the active set and shadow set. AFW uses the Away-step FW and warm start. The dimension indicates the number of variables, where Bound is the number of integer variables. The average time is computed with the geometric mean. # Solved shows the absolute and relative number of instances solved in the time limit of 1800 seconds. All-solved is the average time used on instances that where solved by all different methods.

Sparse Regression	Boscia			SCIP+OA			SCIP+OA Tol 1e-9			Ipopt				
	Dimension	Bound	Instances	Avg Time (s)	# Solved	Relative gap	Avg Time (s)	# Solved	Relative gap	Avg Time (s)	# Solved	Relative gap		
75	3	10	2	10	100%	1.0	0	100%	22.0	0	90%	25	10	100%
80	4	10	12	10	100%	1.0	0	100%	28.0	1	70%	76	9	90%
85	4	10	9	9	90%	1.0	0	100%	29.0	2	60%	75	9	90%
90	4	10	14	10	100%	1.0	0	100%	28.0	7	50%	147	9	90%
95	4	10	11	10	100%	1.0	0	100%	32.0	0	90%	122	8	80%
100	4	10	37	9	90%	1.0	0	100%	31.0	0	80%	147	9	90%
105	5	10	74	9	90%	2.0	0	100%	31.0	4	60%	184	8	80%
110	5	10	137	9	90%	3.0	0	100%	31.0	13	50%	402	8	80%
115	5	10	155	9	90%	3.0	0	100%	36.0	10	50%	506	9	90%
120	5	10	200	9	90%	2.0	0	100%	38.0	28	40%	571	7	70%
125	5	10	178	8	80%	3.0	0	100%	34.0	5	60%	545	8	80%
130	6	10	505	7	70%	3.0	0	100%	40.0	29	40%	1197	5	50%
135	6	10	324	9	90%	3.0	0	100%	40.0	197	30%	809	6	60%
140	6	10	592	6	60%	4.0	0	100%	39.0	83	30%	1158	4	40%
145	6	10	655	5	50%	4.0	0	100%	44.0	647	10%	908	4	40%
150	6	10	795	4	40%	4.0	0	100%	40.0	236	20%	1173	3	30%

Table 8: Comparison of our solver Boscia, outer approximation with SCIP and the interior point solver Ipopt solving sparse regression problems. SCIP+OA Tol 1e-9 is the result for the outer approximation with SCIP and a more restrictive tolerance to generate new cuts, SCIP+OA has a tolerance of 1e-6. The dimension indicates the number of variables, where Bound is the number of integer variables. # Solved shows the absolute and relative number of instances solved in the time limit of 1800 seconds. An instance is considered optimal if the objective value of the solution is close to the minimal value found by any of the three solvers with an absolute tolerance of 1e-4 and a relative tolerance of 1e-2. “_” indicates that there is no instance that could be optimally solved by all.

Sparse Log Regression				Boscia				AFW				No Warm Start				No Active Set				No Shadow Set							
Dimension	Bound	ℓ_{\inf}	var A	Avg Instances	Avg Time (s)	# Solved	All-Solved (s)	Avg Time (s)	# Solved	All-Solved (s)	Avg Time (s)	# Solved	All-Solved (s)	Avg Time (s)	# Solved	All-Solved (s)	Avg Time (s)	# Solved	All-Solved (s)	Avg Time (s)	# Solved	All-Solved (s)	Avg Time (s)				
25	5	0.1	1	3	1	1	3	100%	1	1	3	100%	1	1	3	100%	2	2	3	100%	1	3	100%				
25	5	0.1	5	3	2	2	3	100%	2	2	3	100%	3	3	3	100%	2	2	3	100%	2	2	3	100%			
25	5	1.0	1	3	74	3	100%	36	3	100%	546	3	100%	494	3	100%	65	3	100%	65	3	100%	65	3	100%		
25	5	1.0	5	3	190	129	3	100%	122	90	3	100%	925	664	2	67%	673	2	67%	205	140	3	100%	205	140	3	100%
50	10	0.1	1	3	7	2	3	100%	6	2	3	100%	21	2	2	67%	22	2	2	67%	8	2	3	100%			
50	10	0.1	5	3	83	3	100%	71	71	3	100%	133	133	3	100%	129	3	100%	95	95	3	100%	95	95	3	100%	
50	10	1.0	1	3	1800	-	0%	1800	-	0	0%	1800	-	0	0%	1800	-	0	0%	1800	-	0	0%	1800	-	0	0%
50	10	1.0	5	3	1800	-	0	0%	1800	-	0	0%	1800	-	0	0%	1800	-	0	0%	1800	-	0	0%			
75	15	0.1	1	3	113	0	1	33%	115	0	1	33%	130	1	1	33%	135	1	1	33%	113	0	1	33%			
75	15	0.1	5	3	1257	613	1	33%	1124	438	1	33%	1428	899	1	33%	1433	909	1	33%	1246	597	1	33%			
75	15	1.0	1	3	1800	-	0	0%	1800	-	0	0%	1800	-	0	0%	1800	-	0	0%	1800	-	0	0%			
75	15	1.0	5	3	1800	-	0	0%	1800	-	0	0%	1800	-	0	0%	1800	-	0	0%	1800	-	0	0%			
100	20	0.1	1	3	1800	-	0	0%	1800	-	0	0%	1800	-	0	0%	1800	-	0	0%	1800	-	0	0%			
100	20	0.1	5	3	1800	-	0	0%	1800	-	0	0%	1800	-	0	0%	1800	-	0	0%	1800	-	0	0%			
100	20	1.0	1	3	1800	-	0	0%	1800	-	0	0%	1800	-	0	0%	1800	-	0	0%	1800	-	0	0%			
100	20	1.0	5	3	1800	-	0	0%	1800	-	0	0%	1800	-	0	0%	1800	-	0	0%	1800	-	0	0%			

Table 9: Sparse logistic regression problems solved by using different warm-start and FW methods. Boscia uses the pairwise conditional gradient and warm-start of the active set and shadow set. AFW uses the Away-step FW and warm start. The dimension indicates the number of variables, where Bound is the number of integer variables. The average time is computed with the geometric mean. # Solved shows the absolute and relative number of instances solved in the time limit of 1800 seconds. All-Solved is the average time used on instances that were solved by all different methods. “-” indicates that there is no instance that could be optimally solved by all.

Sparse Log Regression				Boscia				SCIP+OA				Ipopt							
Dimension	Bound	ℓ_{\inf}	var A	Instances	Avg Time (s)	# Solved	Relative gap	Avg Time (s)	# Solved	Relative gap	Avg Time (s)	# Solved	Relative gap	Avg Time (s)	# Solved	Relative gap			
25	5	0.1	1	3	1	3	100%	1.0	0	3	100%	5.0	1.6	3	100%	1.0	1.0	3	100%
25	5	0.1	5	3	2	3	100%	1.0	0	3	100%	92.0	6	3	100%	1.0	1.0	3	100%
25	5	1.0	1	3	74	3	100%	1.0	0	3	100%	22.0	22.1	3	100%	1.0	1.0	3	100%
25	5	1.0	5	3	190	3	100%	1.0	0	3	100%	117.0	30.5	3	100%	1.0	1.0	3	100%
50	10	0.1	1	3	7	3	100%	1.0	0	3	100%	19.0	25.1	1	33%	2.0	2.0	3	100%
50	10	0.1	5	3	83	3	100%	1.0	0	3	100%	169.0	48.9	1	33%	1.0	1.0	3	100%
50	10	1.0	1	3	1800	0	0%	6.0	0	3	100%	32.0	180.0	0	0%	10.0	10.0	3	100%
50	10	1.0	5	3	1800	0	0%	25.0	0	3	100%	165.0	180.0	0	0%	57.0	57.0	3	100%
75	15	0.1	1	3	113	1	33%	5.0	0	3	100%	22.0	68.8	1	33%	1.0	1.0	3	100%
75	15	0.1	5	3	1257	1	33%	54.0	0	3	100%	207.0	180.0	0	0%	Inf	Inf	3	100%
75	15	1.0	1	3	1800	0	0%	53.0	1	3	100%	44.0	180.0	0	0%	12.0	12.0	3	100%
75	15	1.0	5	3	1800	0	0%	39.0	1	3	100%	223.0	180.0	0	0%	92.0	92.0	3	100%
100	20	0.1	1	3	1800	0	0%	9.0	2	3	100%	13.0	180.0	0	0%	Inf	Inf	3	100%
100	20	0.1	5	3	1800	0	0%	115.0	2	3	100%	104.0	180.0	0	0%	7.0	7.0	3	100%
100	20	1.0	1	3	1800	0	0%	21.0	2	3	100%	16.0	180.0	0	0%	63.0	63.0	3	100%
100	20	1.0	5	3	1800	0	0%	215.0	1	3	100%	109.0	180.0	0	0%	63.0	63.0	3	100%

Table 10: Comparison of our solver Boscia, outer approximation with SCIP and the interior point solver Ipopt solving sparse logistic regression problems. The dimension indicates the number of variables, where Bound is the number of integer variables. # Solved shows the absolute and relative number of instances solved in the time limit of 1800 seconds. All-Solved is the average time used on instances that were solved by all three solvers with an absolute tolerance of 1e-4 and a relative tolerance of 1e-2. “-” indicates that there is no instance that could be optimally solved by all.

Tailed Sparse Regression				Boscia				AFW				No Warm Start				No Active Set				No Shadow Set			
n0	m0	ℓ_{inf}	Instances	Avg Time (s)	All-Solved (s)	# Solved	Avg Time (s)	All-Solved (s)	# Solved	Avg Time (s)	All-Solved (s)	# Solved	Avg Time (s)	All-Solved (s)	# Solved	Avg Time (s)	All-Solved (s)	# Solved	Avg Time (s)	All-Solved (s)	# Solved		
5	50	20	10	5	5	10	100%	5	10	100%	5	10	100%	5	10	100%	5	10	100%	5	10	100%	
6	60	20	10	10	10	10	100%	10	10	100%	12	10	100%	12	10	100%	9	10	100%	9	10	100%	
7	70	20	10	21	10	100%	14	14	100%	22	10	100%	24	10	100%	17	10	100%	17	10	100%		
8	80	20	10	33	33	100%	29	10	100%	33	33	100%	33	33	100%	34	10	100%	34	10	100%		
9	90	20	10	84	84	100%	76	76	100%	80	80	100%	86	86	100%	75	10	100%	75	10	100%		
10	100	20	10	162	162	100%	107	107	100%	167	167	100%	185	185	100%	177	10	100%	177	10	100%		
11	110	20	10	326	326	100%	299	299	100%	399	399	100%	390	390	100%	282	10	100%	282	10	100%		
12	120	20	10	689	877	90%	701	471	80%	789	864	80%	709	898	90%	716	821	100%	821	10	100%		
13	130	20	10	1250	-	3	30%	1257	-	5	50%	1271	-	2	20%	1295	-	2	20%	1184	-	3	30%
14	140	20	10	1382	-	2	20%	1800	-	0	0%	1365	-	1	10%	1361	-	1	10%	1343	-	2	20%
15	150	20	10	1413	-	1	10%	1742	-	1	10%	1703	-	1	10%	1619	-	1	10%	1426	-	1	10%

Table 11: Two-tailed sparse regression problems solved by using different warm-start and FW methods. Boscia uses the pairwise conditional gradient and warm-start of the active set and shadow set. AFW uses the Away-step FW and warm start. n0 is the number of variables, m0 is the number of samples. The average time is computed with the geometric mean. # Solved shows the absolute and relative number of instances solved in the time limit of 1800 seconds. All-Solved is the average time used on instances that where solved by all different methods.

Tailed Sparse Regression				Boscia				SCIP+OA					
n0	m0	ℓ_{inf}	Instances	Avg Time (s)	All-Optimal (s)	# Solved	Relative gap	Avg Time (s)	Optimal (s)	All-Optimal (s)	# Solved	Relative gap	
5	50	20	10	5	5	10	100%	0.0	0	0	10	100%	0.0
6	60	20	10	10	9	10	100%	0.0	0	0	10	100%	0.0
7	70	20	10	21	21	10	100%	1.0	0	0	10	100%	1.0
8	80	20	10	33	31	10	100%	1.0	0	0	10	100%	1.0
9	90	20	10	84	82	10	100%	1.0	0	0	10	100%	1.0
10	100	20	10	162	145	10	100%	1.0	0	0	10	100%	0.0
11	110	20	10	326	303	10	100%	1.0	0	0	10	100%	1.0
12	120	20	10	689	603	9	90%	3.0	0	0	10	100%	3.0
13	130	20	10	1250	307	3	30%	102.0	0	0	10	100%	5.0
14	140	20	10	1382	480	2	20%	169.0	0	0	10	100%	52.0
15	150	20	10	1413	160	1	10%	333.0	1	0	10	100%	197.0

Table 12: Comparison of our solver Boscia, outer approximation with SCIP and the interior point solver Ipopt solving two-tailed sparse regression problems. n0 is the number of variables, m0 is the number of samples. The average time is computed with the geometric mean. # Solved shows the absolute and relative number of instances solved in the time limit of 1800 seconds. An instance is considered optimal if the objective value of the solution is close to the minimal value found by any of the three solvers with an absolute tolerance of 1e-4 and a relative tolerance of 1e-2. All-Optimal is the average time used on instances that were solved optimally by all solvers. “-” indicates that there is no instance that could be optimally solved by all.

Tailed Sparse Log Regression			Boscia			AFW			No Warm Start			No Active Set			No Shadow Set			
Dimension	ℓ_{inf}	var A	Avg Instances	Avg Time (s)	All-Solved (s)	Avg Time (s)	All-Solved (s)	# Solved	Avg Time (s)	All-Solved (s)	# Solved	Avg Time (s)	All-Solved (s)	# Solved	Avg Time (s)	All-Solved (s)	# Solved	
10	0.1	1	5	1	1	5	100%	0	0	5	100%	1	5	100%	1	5	100%	
10	0.1	5	5	0	0	5	100%	0	0	5	100%	125	5	100%	133	5	100%	
10	1.0	1	5	1	1	5	100%	1	1	5	100%	3	5	100%	2	5	100%	
10	1.0	5	5	1	1	5	100%	1	1	5	100%	872	294	2	40%	693	166	2
15	0.1	1	5	1	1	5	100%	1	1	5	100%	4	4	100%	4	5	100%	
15	0.1	5	5	1	1	5	100%	1	1	5	100%	156	156	5	100%	148	148	5
15	1.0	1	5	1	1	5	100%	1	1	5	100%	4	4	100%	4	4	100%	
15	1.0	5	5	1	1	5	100%	1	1	5	100%	343	113	3	60%	412	154	3
15	1.0	5	5	1	1	5	100%	1	2	5	100%	6	6	5	100%	6	6	5
20	0.1	1	5	2	2	5	100%	1	1	5	100%	161	161	5	100%	162	162	5
20	0.1	5	5	2	2	5	100%	1	1	5	100%	2	2	5	100%	1	1	5
20	1.0	1	5	2	2	5	100%	2	2	5	100%	7	7	5	100%	7	7	5
20	1.0	5	5	2	2	5	100%	2	2	5	100%	359	240	4	80%	347	230	4
25	0.1	1	5	2	2	5	100%	1	1	5	100%	13	13	5	100%	13	13	5
25	0.1	5	3	3	3	5	100%	1	1	5	100%	357	238	4	80%	388	265	4
25	1.0	1	5	3	3	5	100%	2	2	5	100%	9	9	5	100%	9	9	5
25	1.0	5	3	3	3	5	100%	3	3	5	100%	668	345	3	60%	617	302	3
30	0.1	1	5	3	3	5	100%	2	2	5	100%	15	15	5	100%	15	15	5
30	0.1	5	3	3	3	5	100%	3	3	5	100%	13	13	5	100%	12	12	5
30	0.1	5	3	4	4	5	100%	3	3	5	100%	634	488	4	80%	617	472	4
30	0.1	5	5	3	3	5	100%	6	8	5	100%	779	446	3	60%	883	549	3
30	1.0	5	4	4	5	5	100%	5	4	5	100%	-	-	-	-	4	4	5

Table 13: Two-tailed sparse logistic regression problems solved by using different warm-start and FW methods. Boscia uses the pairwise conditional gradient and warm-start of the active set and shadow set. AFW uses the Away-step FW and warm start. Dimension is the number of data points. The average time is computed with the geometric mean. # *Solved* shows the absolute and relative number of instances solved in the time limit of 1800 seconds. *All-Solved* is the average time used on instances that where solved by all different methods.

Tailed Sparse Log Regression			Boscia			SCIP+DA						
Dimension	ℓ_{inf}	varA	Instances	Avg Time (s)	All-Optimal (s)	# Solved	Relative gap	Avg Time (s)	All-Optimal (s)	# Solved	Relative gap	
10	0.1	1	5	1	1	5	100%	0	22	22	5	100%
10	0.1	5	5	0	0	5	100%	0.0	24	24	5	100%
10	1.0	1	5	5	1	5	100%	0.0	39	39	5	100%
10	1.0	5	5	1	1	5	100%	0.0	38	38	5	100%
15	0.1	1	5	1	1	5	100%	0.0	305	305	5	100%
15	0.1	5	5	1	1	5	100%	0.0	311	311	5	100%
15	1.0	1	5	5	1	5	100%	0.0	519	519	5	100%
15	1.0	5	5	1	1	5	100%	0.0	485	485	5	100%
20	0.1	1	5	2	-	5	100%	0.0	1800	-	0	0%
20	0.1	5	5	2	-	5	100%	0.0	1800	-	0	0%
20	1.0	1	5	5	3	-	5	100%	0.0	1800	-	0
20	1.0	5	5	3	3	-	5	100%	0.0	1800	-	0
25	0.1	1	5	2	2	-	5	100%	0.0	1800	-	0
25	0.1	5	5	2	2	-	5	100%	0.0	1800	-	0
25	0.1	5	5	3	3	-	5	100%	0.0	1800	-	0
25	1.0	1	5	3	3	-	5	100%	0.0	1800	-	0
25	1.0	5	5	3	4	-	5	100%	0.0	1800	-	0
30	0.1	1	5	3	4	-	5	100%	0.0	1800	-	0
30	0.1	5	5	3	4	-	5	100%	0.0	1800	-	0
30	1.0	5	5	4	4	-	5	100%	0.0	1800	-	0

Table 14: Comparison of our solver Boscia, outer approximation with SCIP and the interior point solver Ipopt solving two-tailed sparse logistic regression problems. Dimension is the number of data points. The average time is computed with the geometric mean. # *Solved* shows the absolute and relative number of instances solved in the time limit of 1800 seconds. An instance is considered optimal if the objective value of the solution is close to the minimal value found by any of the three solvers with an absolute tolerance of 1e-4 and a relative tolerance of 1e-2. All-Optimal is the average time used on instances that were solved optimally by all solvers. “-” indicates that there is no instance that could be optimally solved by all.

22433		Boscia		AFW		No Warm Start		No Active Set		No Shadow Set			
vertices	Instances	Avg Time (s)	# Solved	relative gap	Avg Time (s)	# Solved	relative gap	Avg Time (s)	# Solved	relative gap	Avg Time (s)	# Solved	relative gap
4	3	0	3	100%	0.0	0	3	100%	0.0	0	3	100%	0.0
5	3	0	3	100%	0.0	0	3	100%	0.0	0	3	100%	0.0
6	3	0	3	100%	0.0	0	3	100%	0.0	0	3	100%	0.0
7	3	0	3	100%	0.0	0	3	100%	0.0	0	3	100%	0.0
8	3	0	3	100%	0.0	0	3	100%	0.0	0	3	100%	0.0

Table 15: The 22433 MIPLIB instance solved by using different warm-start and FW methods. Boscia uses the pairwise conditional gradient and warm-start of the active set and shadow set. AFW uses the Away-step FW and warm start. *vertices* is the number of vertices of which the sum of distances is minimized. The average time is computed with the geometric mean. *# Solved* shows the absolute and relative number of instances solved in the time limit of 1800 seconds. *All-solved* is the average time used on instances that were solved by all different methods.

22433		Boscia		SCIP+OA		Ipopt							
vertices	Instances	Avg Time (s)	# Solved	relative gap	Avg Time (s)	# Solved	relative gap						
4	3	0	3	100%	0.0	1	3	100%	0.0	129	3	100%	0.0
5	3	0	3	100%	0.0	1	3	100%	0.0	88	3	100%	0.0
6	3	0	3	100%	0.0	1	3	100%	0.0	82	3	100%	0.0
7	3	0	3	100%	0.0	2	3	100%	0.0	175	3	100%	0.0
8	3	0	3	100%	0.0	1	3	100%	0.0	84	3	100%	0.0

Table 16: Comparison of our solver Boscia, outer approximation with SCIP and the interior point solving the 22433 MIPLIB instance. *vertices* is the number of vertices of which the sum of distances is minimized. The average time is computed with the geometric mean. *# Solved* shows the absolute and relative number of instances solved in the time limit of 1800 seconds. An instance is considered optimal if the objective value of the solution is close to the minimal value found by any of the three solvers with an absolute tolerance of 1e-4 and a relative tolerance of 1e-2.

vertices	Instances	Boscia			AFW			No Warm Start			No Active Set			No Shadow Set			
		Avg	Time (s)	# Solved	relative gap	Avg	Time (s)	# Solved	relative gap	Avg	Time (s)	# Solved	relative gap	Avg	Time (s)	# Solved	relative gap
4	3	4	3	100%	1.0	2	3	100%	1.0	2	3	100%	1.0	2	3	100%	1.0
5	3	11	3	100%	1.0	10	3	100%	1.0	12	3	100%	1.0	12	3	100%	1.0
6	3	55	3	100%	1.0	44	3	100%	1.0	64	3	100%	1.0	64	3	100%	1.0
7	3	47	3	100%	1.0	38	3	100%	1.0	61	3	100%	1.0	61	3	100%	1.0
8	3	220	2	67%	3.0	223	2	67%	2.0	241	2	67%	4.0	241	2	67%	4.0

Table 17: The neos5 MIPLIB instance solved by using different warm-start and FW methods. Boscia uses the pairwise conditional gradient and warm-start of the active set and shadow set. AFW uses the Away-step FW and warm start. *vertices* is the number of vertices of which the sum of distances is minimized. The average time is computed with the geometric mean. *# Solved* shows the absolute and relative number of instances solved in the time limit of 1800 seconds. *All-solved* is the average time used on instances that were solved by all different methods.

vertices	Instances	Boscia			SCIP+OA			Ipopt					
		Avg	Time (s)	# Solved	relative gap	Avg	Time (s)	# Solved	relative gap	Avg	Time (s)	# Solved	relative gap
4	3	4	3	100%	1.0	13	3	100%	2.0	3	3	100%	1.0
5	3	11	3	100%	1.0	288	2	67%	1.0	10	3	100%	1.0
6	3	55	3	100%	1.0	643	1	33%	5.0	33	3	100%	1.0
7	3	47	3	100%	1.0	634	2	67%	5.0	24	3	100%	1.0
8	3	220	2	67%	3.0	1800	0	0%	12.0	106	3	100%	3.0

Table 18: Comparison of our solver Boscia, outer approximation with SCIP and the interior point solving the neos5 MIPLIB instance. *vertices* is the number of vertices of which the sum of distances is minimized. The average time is computed with the geometric mean. *# Solved* shows the absolute and relative number of instances solved in the time limit of 1800 seconds. An instance is considered optimal if the objective value of the solution is close to the minimal value found by any of the three solvers with an absolute tolerance of 1e-4 and a relative tolerance of 1e-2.

pg5_34			Boscia			AFW			No Warm Start			No Active Set			No Shadow Set		
vertices	Instances	Avg Time (s)	# Solved	relative gap	Avg Time (s)	# Solved	relative gap	Avg Time (s)	# Solved	relative gap	Avg Time (s)	# Solved	relative gap	Avg Time (s)	# Solved	relative gap	
4	3	1800	0	0%	1.0	1800	0	0%	1.0	1800	0	0%	1.0	1800	0	0%	1.0
5	3	1800	0	0%	1.0	1800	0	0%	1.0	1800	0	0%	1.0	1800	0	0%	1.0
6	3	1800	0	0%	1.0	1800	0	0%	1.0	1800	0	0%	2.0	1800	0	0%	2.0
7	3	1800	0	0%	2.0	1800	0	0%	2.0	1800	0	0%	2.0	1800	0	0%	2.0
8	3	1800	0	0%	2.0	1800	0	0%	2.0	1800	0	0%	3.0	1800	0	0%	3.0

Table 19: The pg5_34 MIPLIB instance solved by using different warm-start and FW methods. Boscia uses the pairwise conditional gradient and warm-start of the active set and shadow set. AFW uses the Away-step FW and warm start. *vertices* is the number of vertices of which the sum of distances is minimized. The average time is computed with the geometric mean. *# Solved* shows the absolute and relative number of instances solved in the time limit of 1800 seconds. *All-solved* is the average time used on instances that were solved by all different methods.

pg5_34			Boscia			SCIP+OA			Ipopt						
vertices	Instances	Avg Time (s)	# Solved	relative gap	Avg Time (s)	# Solved	relative gap	Avg Time (s)	# Solved	relative gap	Avg Time (s)				
4	3	1800	0	0%	1.0	1800	0	0%	13.0	1800	0	0%	Inf	Inf	Inf
5	3	1800	0	0%	1.0	1800	0	0%	Inf	1800	0	0%	Inf	Inf	Inf
6	3	1800	0	0%	1.0	1800	0	0%	Inf	1800	0	0%	Inf	Inf	Inf
7	3	1800	0	0%	2.0	1800	0	0%	Inf	1800	0	0%	Inf	Inf	Inf
8	3	1800	0	0%	2.0	1800	0	0%	Inf	1800	0	0%	Inf	Inf	Inf

Table 20: Comparison of our solver Boscia, outer approximation with SCIP and the interior point solving the pg5_34 MIPLIB instance. *vertices* is the number of vertices of which the sum of distances is minimized. The average time required by a solver is calculated by the geometric mean. *# Solved* shows the absolute and relative number of instances solved in the time limit of 1800 seconds. An instance is considered optimal if the objective value of the solution is close to the minimal value found by any of the three solvers with an absolute tolerance of 1e-4 and a relative tolerance of 1e-2.

ran14x18-disj-8			Boscia			AFW			No Warm Start			No Active Set			No Shadow Set		
vertices	Instances	Avg Time (s)	# Solved	relative gap	Avg Time (s)	# Solved	relative gap	Avg Time (s)	# Solved	relative gap	Avg Time (s)	# Solved	relative gap	Avg Time (s)	# Solved	relative gap	
4	3	1800	0	0%	4.0	1800	0	0%	4.0	1800	0	0%	4.0	1800	0	0%	4.0
5	3	1800	0	0%	5.0	1800	0	0%	8.0	1800	0	0%	5.0	1800	0	0%	5.0
7	3	1800	0	0%	10.0	1800	0	0%	13.0	1800	0	0%	9.0	1800	0	0%	9.0
6	3	1800	0	0%	11.0	1800	0	0%	12.0	1800	0	0%	10.0	1800	0	0%	10.0
8	3	1800	0	0%	25.0	1800	0	0%	28.0	1800	0	0%	21.0	1800	0	0%	21.0

Table 21: The ran14x18-disj-8 MIPLIB instance solved by using different warm-start and FW methods. Boscia uses the pairwise conditional gradient and warm-start of the active set and shadow set. AFW uses the Away-step FW and warm start. *vertices* is the number of vertices of which the sum of distances is minimized. The average time is computed with the geometric mean. *#Solved* shows the absolute and relative number of instances solved in the time limit of 1800 seconds. *All-solved* is the average time used on instances that where solved by all different methods.

ran14x18-disj-8			Boscia			SCIP+OA			Ipopt						
vertices	Instances	Avg Time (s)	# Solved	relative gap	Avg Time (s)	# Solved	relative gap	Avg Time (s)	# Solved	relative gap	Avg Time (s)	# Solved	relative gap		
4	3	1800	0	0%	4.0	1800	0	0%	3.0	1800	0	0%	Inf		
5	3	1800	0	0%	5.0	1800	0	0%	18.0	1800	0	0%	Inf		
7	3	1800	0	0%	10.0	1800	0	0%	21.0	1800	0	0%	Inf		
6	3	1800	0	0%	11.0	1800	0	0%	88.0	1800	0	0%	Inf		
8	3	1800	0	0%	25.0	1800	0	0%	304.0	1800	0	0%	Inf		

Table 22: Comparison of our solver Boscia, outer approximation with SCIP and the interior point solving the ran14x18-disj-8 MIPLIB instance. *vertices* is the number of vertices of which the sum of distances is minimized. The average time required by a solver is calculated by the geometric mean. *#solved* shows the absolute and relative number of instances solved in the time limit of 1800 seconds. An instance is considered optimal if the objective value of the solution is close to the minimal value found by any of the three solvers with an absolute tolerance of 1e-4 and a relative tolerance of 1e-2.

Lasso			Indicator			Big M						
Dimension	Factor	Instances	Avg Time (s)	# Solved	Relative gap	Nodes	LMO calls	Avg Time (s)	# Solved	Relative gap	Nodes	LMO calls
20	2	3	49	3.0	100%	Inf	425	7438	37	3.0	100%	Inf
20	5	3	132	3.0	100%	Inf	1792	30185	151	3.0	100%	Inf
20	10	3	79	3.0	100%	Inf	1070	18417	112	3.0	100%	Inf
50	2	3	1800	0.0	0%	Inf	1747	43474	1787	1.0	33%	Inf
50	5	3	1800	0.0	0%	Inf	3161	80251	1800	0.0	0%	Inf
50	10	3	1800	0.0	0%	Inf	3196	81582	1800	0.0	0%	Inf
70	2	3	1800	0.0	0%	Inf	1053	32141	1800	0.0	0%	Inf
70	5	3	1800	0.0	0%	Inf	1388	42018	1800	0.0	0%	Inf
70	10	3	1800	0.0	0%	Inf	1584	47840	1800	0.0	0%	Inf
100	2	3	1800	0.0	0%	Inf	249	8506	1800	0.0	0%	Inf
100	5	3	1800	0.0	0%	Inf	328	10794	1800	0.0	0%	Inf
100	10	3	1800	0.0	0%	Inf	278	8928	1800	0.0	0%	Inf
150	2	3	1800	0.0	0%	Inf	145	4919	1800	0.0	0%	Inf
150	5	3	1800	0.0	0%	Inf	174	5671	1800	0.0	0%	Inf
150	10	3	1800	0.0	0%	Inf	180	5983	1800	0.0	0%	Inf

Table 23: Comparison of the indicator and the big M formulations for the lasso problem. # *Solved* records the total number of solved instances in the time limit of 1800 seconds. The columns *Nodes* and *LMO calls* show the total number of nodes and LMO calls, respectively.

Sparse Regression			Indicator			Big M						
Dimension	Factor	Instances	Avg Time (s)	# Solved	Relative gap	Nodes	LMO calls	Avg Time (s)	# Solved	Relative gap	Nodes	LMO calls
20	2	3	0	3.0	100%	83.0	4	10	0	3.0	100%	255.0
20	5	3	0	3.0	100%	297.0	1	2	0	3.0	100%	174.0
20	10	3	0	3.0	100%	49.0	1	2	0	3.0	100%	43.0
50	2	3	1800	0.0	0%	22.0	38295	252483	0	3.0	100%	393.0
50	5	3	26	3.0	100%	5.0	892	4508	0	3.0	100%	252.0
50	10	3	0	3.0	100%	3924.0	1	2	0	3.0	100%	381.0
70	2	3	1800	0.0	0%	37.0	26050	184985	384	3.0	100%	15.0
70	5	3	1512	1.0	33%	6.0	29655	195550	0	3.0	100%	363.0
70	10	3	2	3.0	100%	6.0	80	319	0	3.0	100%	265.0
100	2	3	1800	0.0	0%	53.0	7189	51326	1800	0.0	0%	26.0
100	5	3	1800	0.0	0%	14.0	9888	70018	1457	2.0	67%	13.0
100	10	3	282	3.0	100%	2.0	2256	13210	0	3.0	100%	268.0
150	2	3	1800	0.0	0%	84.0	3034	26491	1800	0.0	0%	49.0
150	5	3	1800	0.0	0%	22.0	5243	38223	1800	0.0	0%	21.0
150	10	3	1800	0.0	0%	9.0	8105	52712	1622	1.0	33%	22.0

Table 24: Comparison of the indicator and the big M formulations for the sparse regression problem. # *Solved* records the total number of solved instances in the time limit of 1800 seconds. The columns *Nodes* and *LMO calls* show the total number of nodes and LMO calls, respectively.

Poisson Regression			Indicator			Big M								
Dimension	Factor	Instances	Avg Time (s)	# Solved	Relative gap	Nodes	LMO calls	Avg Time (s)	# Solved	Relative gap	Nodes	LMO calls		
20	2	3	44	3.0	100%	1.0	242	4863	27	3.0	100%	1.0	268	5831
20	5	3	11	3.0	100%	1.0	123	1700	9	3.0	100%	1.0	107	1703
20	10	3	1	3.0	100%	0.0	34	269	1	3.0	100%	1.0	27	247
50	2	3	1800	0.0	0%	51.0	1075	34779	1800	0.0	0%	44.0	683	23935
50	5	3	333	3.0	100%	1.0	1082	17860	918	1.0	33%	4.0	1601	42158
50	10	3	6	3.0	100%	1.0	91	763	10	3.0	100%	1.0	128	1650
70	2	3	88	2.0	67%	18.0	37	471	128	2.0	67%	24.0	35	536
70	5	3	275	1.0	33%	21.0	206	3694	1800	0.0	0%	6.0	711	21206
70	10	3	49	2.0	67%	3.0	200	2217	45	2.0	67%	3.0	107	1748
100	2	3	1800	0.0	0%	190.0	522	9522	1800	0.0	0%	960.0	305	5415
100	5	3	1800	0.0	0%	65.0	528	15165	1800	0.0	0%	41.0	325	10445
100	10	3	259	2.0	67%	2.0	706	9831	197	1.0	33%	3.0	216	4967
150	2	3	54	3.0	100%	121.0	7	56	164	3.0	100%	8.78451279e8	15	110
150	5	3	188	2.0	67%	43.0	28	250	173	2.0	67%	2.22697733e8	18	151
150	10	3	72	3.0	100%	3.0	42	427	219	3.0	100%	5.29980184e8	49	780

Table 25: Comparison of the indicator and the big M formulations for the Poisson regression problem. # *Solved* records the total number and the percentage of solved instances in the time limit of 1800 seconds. The columns *Nodes* and *LMO calls* show the total number of nodes and LMO calls, respectively.

Integer Regression			Indicator			Big M								
Dimension	Factor	Instances	Avg Time (s)	# Solved	Relative gap	Nodes	LMO calls	Avg Time (s)	# Solved	Relative gap	Nodes	LMO calls		
20	2	3	18	3.0	100%	Inf	61	2086	32	3.0	100%	Inf	60	2159
20	5	3	9	3.0	100%	Inf	55	1493	11	3.0	100%	Inf	43	1227
20	10	3	9	3.0	100%	Inf	66	1635	8	3.0	100%	Inf	43	1020
50	2	3	170	3.0	100%	Inf	143	6017	369	3.0	100%	Inf	156	6508
50	5	3	96	3.0	100%	Inf	82	3715	197	3.0	100%	Inf	86	3855
50	10	3	93	3.0	100%	Inf	79	3590	182	3.0	100%	Inf	82	3695
70	2	3	1647	1.0	33%	Inf	405	15584	1800	0.0	0%	Inf	240	8418
70	5	3	565	3.0	100%	Inf	141	6034	1098	3.0	100%	Inf	142	5861
70	10	3	503	3.0	100%	Inf	124	5403	938	3.0	100%	Inf	119	5314
100	2	3	1800	0.0	0%	Inf	337	11243	1800	0.0	0%	Inf	172	5670
100	5	3	1800	0.0	0%	Inf	311	11095	1800	0.0	0%	Inf	171	6142
100	10	3	1800	0.0	0%	Inf	326	12281	1800	0.0	0%	Inf	150	5693
150	2	3	1800	0.0	0%	Inf	227	6568	1800	0.0	0%	Inf	115	3388
150	5	3	1800	0.0	0%	Inf	223	7319	1800	0.0	0%	Inf	115	3838
150	10	3	1800	0.0	0%	Inf	224	7604	1800	0.0	0%	Inf	115	3894

Table 26: Comparison of the indicator and the big M formulations for the integer sparse regression problem. # *Solved* records the total number and the percentage of solved instances in the time limit of 1800 seconds. The columns *Nodes* and *Time (s)* show the total number of nodes and LMO calls, respectively.